

Realizing Predicted Crystal Structures at Extreme Conditions: The Low-Temperature and High-Pressure Crystal Structures of 2-Chlorophenol and 4-Fluorophenol

Iain D. H. Oswald,[†] David R. Allan,[†] Graeme M. Day,^{*,‡}
W. D. Samuel Motherwell,[§] and Simon Parsons^{*,†}

School of Chemistry and The Centre for Science at Extreme Conditions, The University of Edinburgh, King's Buildings, West Mains Road, Edinburgh EH9 3JJ, Scotland, Pfizer Institute for Pharmaceutical Materials Science, Department of Chemistry, University of Cambridge, Lensfield Road, Cambridge CB2 1EW, England, and Cambridge Crystallographic Data Centre, 12 Union Road, Cambridge CB2 1EZ, England

Received October 14, 2004

ABSTRACT: A crystal of 2-chlorophenol was grown from the liquid at ambient pressure by laser-assisted zone refinement; 4-fluorophenol was crystallized from ethanol. Different polymorphs were obtained at high pressure by compression of the liquids in a Merrill-Bassett diamond-anvil cell (crystallization pressures 0.12 and 0.28 GPa, respectively). The structures of all phases are characterized by OH...OH hydrogen-bond formation. In the ambient-pressure polymorph of 2-chlorophenol, a hydrogen-bonded chain is formed about a 3_2 screw-axis; the ambient-pressure phase of 4-fluorophenol contains hexameric rings located on $\bar{3}$ sites. In crystallizing in high-symmetry space groups, these two compounds conform to typical behavior for bulky monoalcohols. By contrast, at high-pressure both compounds form zigzag chains disposed about 2_1 screw-axes, behavior more characteristic of small monoalcohols. The halophenol moiety thus behaves as a bulky group at ambient pressure but a small group at high pressure. We show that Crystal Structure Prediction methodologies reproduce all four phases, even though the potentials used were developed using ambient-pressure data. This is especially encouraging as the ambient-pressure phase of 2-chlorophenol contains three molecules in the asymmetric unit, while the high-pressure phase of 4-fluorophenol is disordered.

Introduction

In 1999 and 2001, the Cambridge Crystallographic Data Centre held two blind tests of crystal structure prediction (CSP1999 and CSP2001).^{1,2} The aim of these projects was to test how well currently available methods of crystal structure prediction perform when given only the atomic connectivity for an organic compound. Several groups active in the field of crystal structure prediction attempted to predict the crystal structures of compounds of varying size and flexibility. The crystal structures were all previously unpublished, contained less than 40 atoms and crystallized in a common space group with $Z' = 1$. All predictions were carried out with no consideration of pressure. The results of the tests showed that rigid molecules are most amenable to crystal structure prediction, the authors concluding that, 'Crystal structure prediction, although beset by fundamental and technical difficulties, is no longer scandalously hopeless.'

Most of the subjects used for the crystal structure prediction blind tests had only been characterized in one polymorphic form, though it is well-known that many organic systems may crystallize as different polymorphs under different conditions. The observed structures were thus not guaranteed to be the most thermodynamically

stable. This must have relevance with regard to the predictability of their crystal structures, as most prediction methodologies aim to locate the global minimum in lattice energy as the most probable crystal structure. A frequent observation in crystal structure prediction studies is that there are many possible crystal structures within a small energy range of the global minimum in lattice energy (CSP1999 and CSP2001).^{1,2} While the calculations usually locate many more potential polymorphs than are likely to ever be observed, it seems likely that some of the previously unobserved structures from these studies should be accessible through changes in the crystallization conditions.

Previous results from this laboratory have shown that high pressure (0.1–10 GPa) is a powerful means for investigating polymorphism in organic systems. We have characterized, for example, new high-pressure phases in alcohols,^{3–6} carboxylic acids,^{4,7} acetone,⁸ and, very recently, glycine⁹ and serine.¹⁰ The area is still relatively underdeveloped, however, and systematic trends are still emerging.

Computational studies of isolated molecules have had an enormous influence on the development of structural chemistry, and it is thus of great interest to test the effectiveness of computational approaches to the prediction of high-pressure crystal structures. It is not immediately obvious that potentials developed for ambient-pressure calculations should be satisfactory at high pressures. Even if the electron distribution of a molecule is unaffected by high pressures, most model potentials are empirically parametrized to reproduce properties of ambient pressure crystals. High pressure will sample

* To whom correspondence should be addressed. Dr. S. Parsons, School of Chemistry, The University of Edinburgh, King's Buildings, West Mains Road, Edinburgh EH9 3JJ, Scotland. Tel: 0131 650 5804. Fax: 0131 650 4743. E-mail: S.Parsons@ed.ac.uk.

[†] The University of Edinburgh.

[‡] University of Cambridge.

[§] Cambridge Crystallographic Data Centre.

Table 1. Crystallographic Data for 2-Chlorophenol and 4-Fluorophenol at Both Ambient and High Pressure

	compound			
	2-chlorophenol-I	2-chlorophenol-II	4-fluorophenol-I	4-fluorophenol-II
<i>T/P</i>	100 K/0 GPa	RT/0.12 GPa	150 K/0 GPa	RT/0.28 GPa
formula	C ₆ H ₆ ClO	C ₆ H ₆ ClO	C ₆ H ₆ FO	C ₆ H ₆ FO
weight	128.56	128.56	112.10	112.10
radiation	Mo–K α	Mo–K α	Mo–K α	Mo–K α
crystal system	trigonal	monoclinic	trigonal	monoclinic
space group	<i>P</i> 3 ₂	<i>P</i> 2 ₁ / <i>n</i>	<i>R</i> 3	<i>P</i> 2 ₁ / <i>n</i>
<i>a</i> , Å	16.0721(8)	6.4638(12)	22.620(2)	6.2807(7)
<i>b</i> , Å	16.0721(8)	4.9086(4)	22.620(2)	5.7241(9)
<i>c</i> , Å	5.8959(6)	18.131(3)	5.5690(11)	7.7982(12)
α , deg	90	90	90	90
β , deg	90	98.111(13)	90	106.060(11)
γ , deg	120	90	120	90
volume, Å ³	1318.94(16)	569.49(15)	2467.8(6)	269.41(7)
no. reflns for cell	8931	539	1550	268
$2\theta_{\max}$ (deg)	57.87	52.79	57.86	46.43
<i>Z</i>	9	4	18	2
<i>D_c</i> (mg/m ³)	1.457	1.499	1.358	1.382
μ (mm ⁻¹)	0.534	0.550	0.114	0.166
reflns collected	11871	3522	5190	764
unique [<i>R</i> _{int}]	3901 [0.026]	426 [0.087]	1349 [0.019]	201 [0.032]
no. <i>I</i> > 2 <i>u</i> (<i>I</i>)	3738	249	955	132
<i>T</i> _{min} / <i>T</i> _{max}	0.44/0.76	0.58/0.91	0.97/0.98	0.62/0.97
params	227	31	76	29
<i>R</i> ₁ [<i>F</i> > 4 <i>u</i> (<i>F</i>)]	0.0274	0.0679	0.0469	0.1060
<i>wR</i> ₂ (<i>F</i> ² , all data)	0.0704	0.1320	0.0837	0.3031
<i>S</i>	0.9947	1.0517	1.1435	1.3200
$\Delta\rho_{\max}$, e Å ⁻³	0.27	0.34	0.48	0.39
$\Delta\rho_{\min}$, e Å ⁻³	-0.24	-0.30	-0.40	-0.17

atom–atom potentials at generally shorter separations than are represented in the structures used for this parametrization. High-pressure phases have higher densities than their ambient-pressure counterparts, and, as there is often a reasonable variation of densities among the lowest energy predicted structures for a given molecule,^{11,12} the application of pressure could reorder their thermodynamic stability. Thus, it seems possible that the highest density predicted crystal structures could in fact be accessible at high-pressure.

The compounds selected for our first investigation to test this idea were the mono-halophenols. Crystal structures in this series have only been lightly investigated: 4-chlorophenol was studied by Perrin and Michel^{13,14} and shown to exist in two polymorphic forms. However, these systems are ideal for structure prediction tests because the molecules are small and rigid. The compounds are mostly liquids under ambient pressure, and so in situ crystal growth by application of pressure can yield new polymorphs directly, avoiding the complications which can arise by applying pressure to a solid sample. They are also a good test of the two major aspects of prediction methodologies: the location of all possible crystal structures and the calculation of their relative energies. Results of the latest crystal structure prediction blind test¹⁵ highlighted the prediction of structures with *Z'* > 1 as a major challenge for the search methodologies. Monoalcohols have a tendency to crystallize with more than one molecule in the asymmetric unit, so a complete search for structures must include *Z'* > 1. Furthermore, the strong orientational dependence of close contacts with halogen atoms presents problems for atomistic calculations and their presence tests the quality of interatomic potentials that have recently been developed for these atoms.

In this paper we describe the crystal structures of two halophenols, 2-chlorophenol and 4-fluorophenol, that

exhibit pressure induced polymorphism and also describe the results of crystal structure prediction calculations on the two systems. We have described the crystal structures of the other monofluoro- and monochlorophenols elsewhere.¹⁶

Experimental Section

General Procedures. 2-Chlorophenol and 4-fluorophenol were obtained from Sigma-Aldrich and used as received.

X-ray diffraction intensities were collected with Mo–K α radiation on a Bruker SMART APEX CCD diffractometer equipped with an Oxford Cryosystems low-temperature device¹⁷ and an OHCD laser-assisted crystal growth device.

Crystal Growth at Ambient Pressure. 2-Chlorophenol (mp 280 K) was drawn into a glass capillary (o.d. 0.52 mm) and flame-sealed. The sample was mounted on the diffractometer, and a polycrystalline mass obtained by freezing the sample at 273 K. A crystal was grown using the laser-assisted zone-refinement procedure of Boese and Nussbaumer.¹⁸

Colorless crystals were grown from a saturated solution of 4-fluorophenol (mp 321 K) in ethanol at 277 K.

Crystal Structure Determination of Ambient-Pressure Phases. Diffraction data were collected for 2-chlorophenol at 100 K and for 4-fluorophenol at 150 K. Data collection and integration were carried out using the programs SMART¹⁹ and SAINT.²⁰ The diffraction data were corrected for absorption and other systematic errors using the multiscan procedure SADABS.^{21,22} The structure was solved by direct methods (SIR92)²³ and refined by full-matrix least squares against *F*² using all data (CRYSTALS).²⁴ H-atoms were placed on C-atoms in calculated positions and allowed to ride on their parent atoms. Hydroxyl hydrogen atoms were located in difference maps and refined with a distance restraint of 0.85 Å to the parent oxygen. All non-H atoms were modeled with anisotropic displacement parameters. In the case of 2-chlorophenol the value of the Flack parameter [0.00(3)]²⁵ verified the correct assignment of the absolute structure. Data collection and refinement statistics are collected in Table 1. We refer to the low-temperature phases as 2-chlorophenol-I and 4-fluorophenol-I.

Crystal Growth at High Pressure. Pressure was applied to the samples using a Merrill-Bassett diamond anvil cell (DAC) equipped with 600 μm culets, a tungsten gasket with a 300 μm hole, beryllium backing disks and a chip of ruby for pressure measurement.²⁶ Pressures were measured by the ruby-fluorescence method by excitation with a 632.817 nm line from a He–Ne laser using a Jobin-Yvon LabRam 300 Raman spectrometer.

2-Chlorophenol and 4-fluorophenol were loaded into the Merrill-Bassett cell as liquids. In the case of 4-fluorophenol, both the sample and the cell were heated with a hot-air gun before loading to prevent crystallization at ambient temperature. In each case, the cell was closed, and pressure was applied until a polycrystalline mass was produced; the temperature of the cell was increased using a hot-air gun until a single crystallite remained. Slow cooling to ambient temperature yielded a single crystal that filled the entire gasket hole. Crystallization was monitored visually using a polarizing microscope. The crystallization pressures were 0.12 GPa for 2-chlorophenol and 0.28 GPa for 4-fluorophenol.

Structure Determinations of 2-Chlorophenol and 4-Fluorophenol at High Pressure. Data were collected with the cell mounted in two different orientations for 2-chlorophenol but only one for 4-fluorophenol; the diffraction pattern was indexed with the program GEMINI.²⁷ Data integration (to $2\theta = 45^\circ$) was performed using SAINT with dynamic masking to account for the shading from the DAC steel body. The program SHADE²⁸ was used to take account absorption effects of the pressure cell; further systematic errors were treated using SADABS before merging in SORTAV.²⁹ More detailed data collection and processing procedures used in our laboratory have been described in ref 30.

Indexing the diffraction patterns showed that the phases obtained at high pressure were different from those obtained on cooling. We refer to the high-pressure phases as 2-chlorophenol-II and 4-fluorophenol-II.

High-pressure data sets obtained by applying DAC techniques to crystals in low-symmetry crystal systems have a low completeness because of shading by the cell-body. This is exacerbated if a crystal happens to grow in an unfavorable orientation inside the cell, and there is very little that can be done to control this. In the case of 2-chlorophenol the completeness obtained was just 37%, and this meant that structure solution by direct methods failed to yield a recognizable solution, while Patterson methods were frustrated by the elongation of the peaks in the direction most affected by pressure-cell shading. This is a common problem with high-pressure data, but fortunately the problem may be overcome by using global optimization methods originally devised for structure solution from powder diffraction data.³¹ The structure of phase-II of 2-chlorophenol was solved using the simulated annealing procedure in the program TOPAS.³² The structure refined by full-matrix least-squares against F^2 (CRYSTALS). Free refinement of the positional parameters of the non-H atoms yielded carbon–carbon bond lengths varying from 1.34 to 1.40 Å. The phenyl ring was therefore constrained to be a rigid hexagon. H-atoms were placed on C-atoms in calculated positions and allowed to ride on their parent atoms. The hydroxyl hydrogen atom, which is involved in H-bonding, was located in a difference map; its position was initially refined subject to distance and angular restraints, but later fixed. The final R -factor calculated on F for data with $I/u(I) > 2.0$ was 8.12%.

The structure of the 4-fluorophenol-II was solved by direct methods (SIR92). The molecule occupies an inversion center with the oxygen and fluorine disordered. The structure was refined by similar procedure to those described above. All non-H atoms were modeled with anisotropic displacement parameters that were subject to thermal and vibrational restraints. The carbon–carbon bond lengths are slightly shorter than is expected, possibly because of librational motion of the ring. The displacement parameter for C3 is slightly elongated along the bond, which supports this hypothesis. The

final R -factor calculated on F for data with $I/u(I) > 2.0$ was 10.60%. Final data collection and refinement statistics are collected in Table 1.

Interconversion of 4-Fluorophenol-I and II. The high melting-point of 4-fluorophenol (321 K) in principle means that crystals formed at high pressure may be recoverable at ambient pressure without the sample melting. In the event an attempt to release the pressure on the sample of 4-fluorophenol transformed the crystal into a polycrystalline mass, suggesting that the solid underwent a destructive phase transition, presumably to the ambient-pressure phase.

A single crystal of 4-fluorophenol-I (prepared at ambient pressure as described above) was loaded into the Merrill-Bassett cell with paraffin as a hydrostatic medium. Pressure (1.7 GPa) was applied, and data collected as described above. The sample indexed on phase-I of 4-fluorophenol though the diffraction data were very weak. The unit cell dimensions were: $a = 21.387(3)$, $c = 5.5660(17)$ Å, which compares to 22.620(2) and 5.5690(11) Å at ambient pressure and 100 K. The structure of phase-I refined to $R1 = 8.9\%$ based on 146 data out of 346 with $I > 2u(I)$. The appearance of the crystal changed overnight from being transparent to having regions where the crystal had become opaque, suggesting that the sample was becoming polycrystalline. The Raman spectrum of the polycrystalline material showed a band with some indication of a shoulder at 847 cm^{-1} (Figure 1). The Raman spectrum of phase-I contains a prominent doublet in this region, whereas that of phase-II consists of one strong peak with a smaller peak to high frequency. On this basis it is possible that the polycrystalline material is 4-fluorophenol-II, though this is a rather tentative conclusion.

Intriguingly, on release of pressure, the crystal became transparent and was identified as a single crystal of 4-fluorophenol-I (by single-crystal diffraction methods). The behavior described above was reproducible for the same sample. Increasing the pressure on the single-crystal resulted in growth of polycrystalline regions; release of pressure returned the crystal to its original condition.

Software and Other General Crystallographic Procedures. The structures were visualized using SHELXTL-XP³³ or MERCURY;³⁴ the figures were produced using CAMERON.³⁵ Other analysis utilized the p.c. version of PLATON.^{36,37} Searches of the Cambridge Structural Database were carried out with the program CONQUEST, utilizing version 5.25 of the database.^{38,39} Crystallographic information files for all structures reported here are available in the Supporting Information. The numbering scheme used is shown in Scheme 1. Intermolecular H-bonding interactions have been summarized in Table 2.

Computational Details

The crystal structure prediction part of this study was performed separately from the experimental crystallizations. In keeping the prediction “blind” from the experimental results, the only information about the observed crystals known in advance of the computational work was that two forms were isolated for each molecule, all crystallizing with three or fewer molecules in the asymmetric unit. As the choice of space groups is crucial for the success of crystal structure prediction, it was also revealed that at least one form crystallizes in a trigonal space group. Searches were performed for low energy crystal structures of 2-chlorophenol and 4-fluorophenol using the simulated annealing search method^{40–42} implemented in the Cerius2 modeling package.⁴³ Planar, rigid molecular structures were used throughout the modeling. Two planar conformations of the 2-chlorophenol molecule are possible, so the Cambridge Structural Database was searched for structures with neighboring hydroxyl and chloro- substituents on

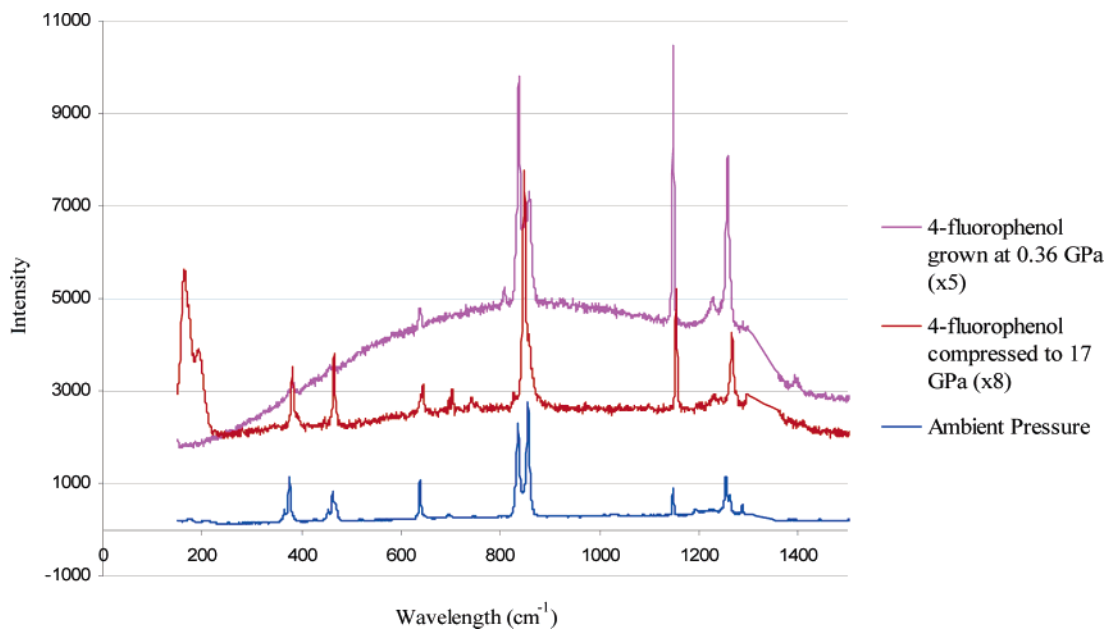
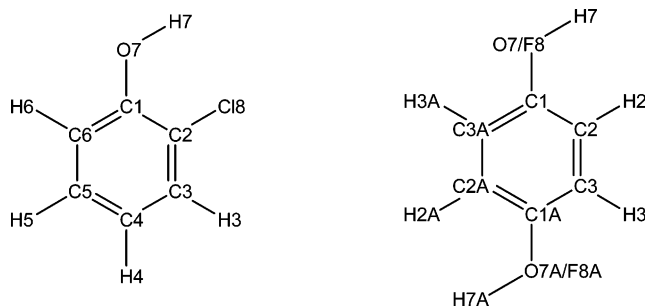


Figure 1. Raman spectra of 4-fluorophenol under various conditions; solid, phase-I at ambient pressure (blue line); phase-I compressed to 1.7 GPa and allowed to become polycrystalline over the course of 2 days (red line); phase-II grown from the melt at 0.36 GPa (pink line).

Scheme 1. Conventional Structure Diagram and Numbering Scheme for 2-Chlorophenol and 4-Fluorophenol^a



^a 4-Fluorophenol is disordered over an inversion center; hence, those atoms augmented by an A are generated by inversion symmetry.

aromatic rings. In almost all cases where hydrogen positions are reported, the hydroxyl hydrogen points away from the chlorine atom; we therefore assumed the chlorophenol conformation with hydroxyl pointing away from the chlorine atom. Molecular structures were taken from density functional theory optimizations, using the VWN-BP functional⁴⁴⁻⁴⁶ and the DNP numerical basis set within the program DMol3.⁴⁷

The initial searches for low energy crystal structures were performed using the *exp-6* model potential parameters for C, H, and O fitted to hydrocarbons⁴⁸ and oxohydrocarbons,⁴⁹ and parameters for chlorine and fluorine fitted to perchlorohydrocarbons⁵⁰ and perfluorohydrocarbons.⁵¹ For this model, all C-H and O-H bonds were foreshortened by 0.1 Å, moving the interaction site for hydrogen atoms away from the nucleus, toward the true maximum in charge density. For both molecules, the electrostatics were modeled by atomic charges fitted to the quantum chemically calculated (DFT) electrostatic potential. This *exp-6* + atomic charge model is limited by the assumption that the interaction

between atoms is independent of orientation. This isotropic atom approximation can seriously limit the accuracy of crystal structure modeling, especially for the electrostatic interactions in hydrogen bonded crystals and the close contacts with halogen atoms. Hence, for final lattice energy minimizations, we replaced the atomic point charges with an atomic multipole model, calculated from a DFT wave function using the B3P91 functional and 6-31G(*d,p*) basis set. This calculation was performed within the program CADPAC⁵² and multipoles, up to hexadecapole (i.e. charge, dipole, quadrupole, octupole, and hexadecapole) were derived using a distributed multipole analysis (DMA).^{53,54}

In the final energy minimizations of the predicted 4-fluorophenol structures, we kept the spherical atom *exp-6* model used in the initial search. However, including anisotropy in the repulsive wall around chlorine atoms appears to be crucially important for modeling crystals of chlorinated molecules.^{55,56} We therefore used a more elaborate model for the repulsion and dispersion interactions in the final energy minimizations of 2-chlorophenol crystal structures. Recent advances in models for intermolecular interactions involving chlorine atoms have led to successful crystal structure predictions for other chlorinated aromatic molecules,^{56,57} so we adapted a nonempirical model potential originally derived for chlorobenzenes.⁵⁶ The model has the *exp-6* form for repulsion and dispersion interactions, allowing for anisotropy in the repulsive wall through an orientation-dependent term in the exponential:

$$U = \sum_{i \in M, k \in N} [A^{ik} \exp(-\alpha^{ik} [R_{ik} - \rho(\Omega_{ik})]) - C_6^{ik}/R_{ik}^6 + U_{\text{elec}}(\text{DMA}, \Omega_{ik}, R_{ik}^{-n}, n \leq 5)] \quad (1)$$

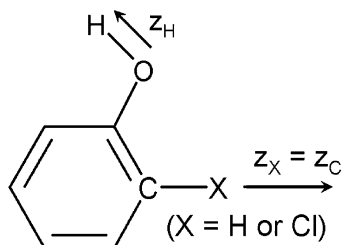
$$\rho^{ik}(\Omega) = \rho_1^i(\hat{\mathbf{z}}_i \cdot \hat{\mathbf{R}}_{ik}) + \rho_1^k(-\hat{\mathbf{z}}_k \cdot \hat{\mathbf{R}}_{ik}) + \rho_2^i(3[\hat{\mathbf{z}}_i \cdot \hat{\mathbf{R}}_{ik}]^2 - 1)/2 + \rho_2^k(3[\hat{\mathbf{z}}_k \cdot \hat{\mathbf{R}}_{ik}]^2 - 1)/2 \quad (2)$$

Table 2: Table of Hydrogen Bonding Parameters^a

compound			low <i>T</i>	high <i>P</i>
2-chlorophenol-I	O71	O71 ⁱ	2.754(2)	
	O72	O72 ⁱⁱ	2.748(1)	
	O73	O73 ⁱⁱⁱ	2.762(2)	
	H42	Cl81 ^{iv}	2.89	
	H52	Cl81 ^v	2.94	
	H43	Cl82 ⁱⁱ	2.88	
	H53	Cl82 ^{vi}	2.81	
2-chlorophenol-II	O7	O7 ^{vii}		2.809(11)
	H3	Cl8 ^{viii}		2.98
4-fluorophenol-I	O7	O7 ^{ix}	2.650(1)	
	H2	F8 ^x	2.57	
	H5	F8 ^{xi}	2.65	
4-fluorophenol-II	O7	O7 ^{xii}		3.017(4)

^a The H-bonding distances are in Å. Low-temperature datasets were taken at 100 and 150 K for 2-chlorophenol and 4-fluorophenol, respectively. The high-pressure datasets were collected at room temperature. (i) $-y, x - y, z - 1/3$; (ii) $1 - y, x - y, z - 1/3$; (iii) $-y, x - y - 1, z - 1/3$; (iv) $-x + y, -x, 1/3 + z$; (v) $-x + y, -x, z - 2/3$; (vi) $1 - y, x - y, 2/3 + z$; (vii) $3/2 - x, y - 1/2, 1/2 - z$; (viii) $2 - x, -y, -z$; (ix) $1 + y, 1 - x + y, 2 - z$; (x) $4/3 - y, x - y - 1/3, 2/3 + z$; (xi) $5/3 - x, 1/3 - y, 1/3 - z$; (xii) $-x - 1, y - 1/2, -z - 1/2$.

Scheme 2. Atomic Axes Used in the Anisotropic Repulsion Model



Here, \mathbf{R}_{ik} is the distance between atoms i and k , of type ι and κ , in molecules M and N ; $\hat{\mathbf{R}}_{ik}$ is the corresponding unit vector and $\hat{\mathbf{z}}_k$ is the unit vector along the atomic z -axis. Ω_{ik} represents the relative orientation of atoms i and k . The atomic axes for this model are shown in Scheme 2. The model used for repulsion anisotropy (eq 2) includes dipolar and quadrupolar type terms, both of which have cylindrical symmetry about the z -axis.

For carbon, chlorine and the hydrogen atoms bonded to carbon, parameters were taken directly from ref 56

Table 3. Final Parameters of the 2-Chlorophenol Model Potential^a

atom types		$A^{\iota\kappa}$, kJ mol ⁻¹	$B^{\iota\kappa}$, Å ⁻¹	$C_6^{\iota\kappa}$, Å ⁶ kJ mol ⁻¹	ρ_1^{ι} , Å	ρ_2^{ι} , Å	ρ_1^{κ} , Å	ρ_2^{κ} , Å
ι	κ							
Cl	Cl	569746	3.3427	8366.9	+0.0156	+0.0156	-0.0939	-0.0939
C _{Cl}	C _{Cl}	28957	3.2131	2146.4	-0.2054	-0.2054	-0.3109	-0.3109
C _{H/O}	C _{H/O}	107333	3.1936	2146.4	-0.0026	-0.0026	+0.0419	+0.0419
O	O	94728	3.4600	1221.8	0.0	0.0	0.0	0.0
H _C	H _C	2220	3.2575	200.0	-0.0449	-0.0449	+0.0036	+0.0036
H _O	H _O	673	3.6900	15.1	-0.0449	-0.0449	0.0	0.0
Cl	C _{Cl}	277307	3.5474	4234.3	+0.0156	-0.2054	-0.0939	-0.3109
Cl	C _{H/O}	219400	3.2465	4234.3	+0.0156	-0.0026	-0.0939	+0.0419
Cl	O	232316	3.4014	3176.5	+0.0156	0.0	-0.0939	0.0
Cl	H _C	30829	3.2597	1293.1	+0.0156	-0.0449	-0.0939	+0.0036
Cl	H _O	19575	3.5163	355.6	+0.0156	-0.0449	-0.0939	0.0
C _{Cl}	C _H	61374	3.2443	2146.4	-0.2054	-0.0026	-0.3109	+0.0419
C _{Cl}	O	52378	3.3365	1608.9	-0.2054	0.0	-0.3109	0.0
C _{H/O}	O	100838	3.3268	1608.9	-0.0026	0.0	+0.0419	0.0
C _{Cl}	H _C	11254	3.3709	653.7	-0.2054	-0.0449	-0.3109	+0.0036
C _{Cl}	H _O	4413	3.4515	180.1	-0.2054	-0.0449	-0.3109	0.0
C _{H/O}	H _C	16950	3.2654	653.7	-0.0026	-0.0449	+0.0419	+0.0036
C _{H/O}	H _O	8497	3.4418	180.1	-0.0026	-0.0449	+0.0419	0.0
H _C	H _O	1222	3.4738	55.0	-0.0449	-0.0449	+0.0036	0.0

^a C_{Cl} is a carbon bonded to chlorine. C_{H/O} is a carbon bonded to hydrogen or oxygen. H_C is a hydrogen bonded to carbon. H_O is a hydroxyl hydrogen. Atomic z -axes are defined along the bonds pointing out from the aromatic ring (Scheme 2).

and parameters for oxygen and the hydroxyl hydrogen were empirically fitted to reproduce the known crystal structures and sublimation enthalpies of a set of similar molecules: resorcinol, 3,4-dichlorophenol, 3,5-dichlorophenol and tetrachlorohydroquinone. No anisotropy was used for the repulsion on oxygen atoms, while the ρ_1 coefficients from H_C hydrogen atoms were transferred to the hydroxyl hydrogen. This anisotropic term accounts for the shift of electron density away from the nucleus on hydrogen atoms and has a similar effect to the X-H bond foreshortening that was used with the isotropic *exp-6* model. The final parameters are given in Table 3.

In most crystal structure prediction studies, it is common to search only the most common space groups; approximately 95% of homomolecular organic crystal structures are found in fewer than 10 space groups. In this work, we knew in advance that one of the polymorphs of 2-chlorophenol crystallizes in a trigonal space group. Therefore, in addition to the most common space groups for organic molecular crystals, the most common trigonal space groups were also searched (Table 4). Furthermore, we did not limit our search to having one molecule in the asymmetric unit; monoalcohols sometimes crystallize with $Z' > 1$ to optimize their hydrogen bonding, so we searched for crystals with one, two and three molecules in the asymmetric unit. The computing time was only available to repeat the simulated annealing search 4 times for each of these space group/ Z' combinations. Four repeats usually results in a complete search in $Z' = 1$,⁵⁸ but we risk missing some low energy structures with $Z' = 2$ and 3.

All structures within 15 kJ mol⁻¹ of the global minimum from the search with the simple model potential were then re-minimized using the more elaborate anisotropic model within the program DMAREL.^{59,60} All terms up to R^{-5} in the multipole expansion were included in the calculation of electrostatic energies, using Ewald summation for charge-charge, charge-dipole and dipole-dipole interactions, and direct summation to a 15 Å cutoff between molecular centers of mass for the higher order terms. All structures were

Table 4. Space Groups Searched during Crystal Structure Prediction Calculations

	most common space groups searched	trigonal space groups searched
$Z' = 1$	$P2_1/c, P\bar{1}, P2_12_12_1, P2_1, C2/c, Pbca, Pnma, Pna2_1, Pbcn$	$P\bar{3}, P3_12_1 (P3_22_1), R\bar{3}, P3, P3_1 (P3_2), R3, R3c$
$Z' = 2$	$P2_1/c, P\bar{1}, P2_12_12_1, P2_1, C2/c, P1$	$P\bar{3}, P3_12_1 (P3_22_1), R\bar{3}, P3, P3_1 (P3_2), R3, R3c$
$Z' = 3$	$P2_1/c, P\bar{1}, P2_12_12_1, P2_1, C2/c, P1$	$P\bar{3}, P3_12_1 (P3_22_1), R\bar{3}, P3, P3_1 (P3_2), R3, R3c$

energy-minimized using symmetry constraints, then tested for stability by calculating ($\mathbf{k} = 0$) phonon frequencies and the elastic stiffness matrix. Any structures with instabilities were pushed away from saddle points and re-minimized with all symmetry constraints removed. The final energy minimized structures were clustered using the COMPACT program⁶¹ to remove repeats of identical structures.

Results

Pressures of a few tenths of a GPa are unlikely to affect intramolecular geometry significantly, and intramolecular distances and angles in the refinements of the high-pressure structures were restrained to be equal to those observed at low-temperature. This is often necessary in high-pressure work to control the effects of low data completeness, and it means that comparison of intramolecular geometry at high and ambient pressures is not possible. It is the effect of pressure on intermolecular geometry and crystal packing which we address in this paper. Intermolecular H-bonding interactions have been summarized in Table 2.

2-Chlorophenol at 100 K. Phase-I of 2-chlorophenol crystallizes at low-temperature in the trigonal space

group $P3_2$ with three molecules in the asymmetric unit; in the accompanying tables these molecules are numbered C11–Cl81, C12–Cl82, C13–Cl83, and are referred to as molecules 1, 2 and 3 below (see also Scheme 1). The bond distances and angles are normal, and do not differ between the components of the asymmetric unit. The molecules interact via $\cdots\text{OH}\cdots\text{OH}\cdots$ H-bonds to form helices disposed about crystallographic 3_2 screw-axes, conforming to a $C(2)$ graph set (Figure 2). Each helix is composed of crystallographically equivalent molecules. All the hydrogen bonds are of similar strength: the distances $\text{O}7x\cdots\text{O}7x'$ measure 2.754(2), 2.748(1) and 2.762(2) Å for $x = 1, 2$ and 3, respectively.

$\text{H}\cdots\text{Cl}$ contacts are formed between the helices composed of molecules 1 and 2 and 2 and 3; there are no contacts between molecules 1 and 3. In each case the chlorine of one helix interacts with two hydrogen atoms from the other helix. The contact distances (Å) are: $\text{Cl}(81)\cdots\text{H}(42)$ 2.89 and $\text{Cl}(81)\cdots\text{H}(52)$ 2.94; $\text{Cl}(82)\cdots\text{H}(43)$ 2.88 and $\text{Cl}(82)\cdots\text{H}(53)$ 2.81 Å. The sum of the van der Waals radii of H and Cl is 2.95 Å, though this has been criticized as a criterion for assessing the importance of hydrogen bonds.⁶² Figure 2 shows the hydrogen bonding and close contacts in the structure, but, for clarity, only the shortest contact between two groups has been labeled.

2-Chlorophenol at 0.12 GPa. Phase-II of 2-chlorophenol was obtained on crystallization from the liquid at 0.12 GPa. The structure crystallizes in space group $P2_1/n$ with one molecule in the asymmetric unit. As in phase-I, the molecules interact via $\cdots\text{OH}\cdots\text{OH}\cdots$ hydrogen bonds, forming $C(2)$ chains, but by contrast to phase-I, where helices were formed, these chains zigzag about a

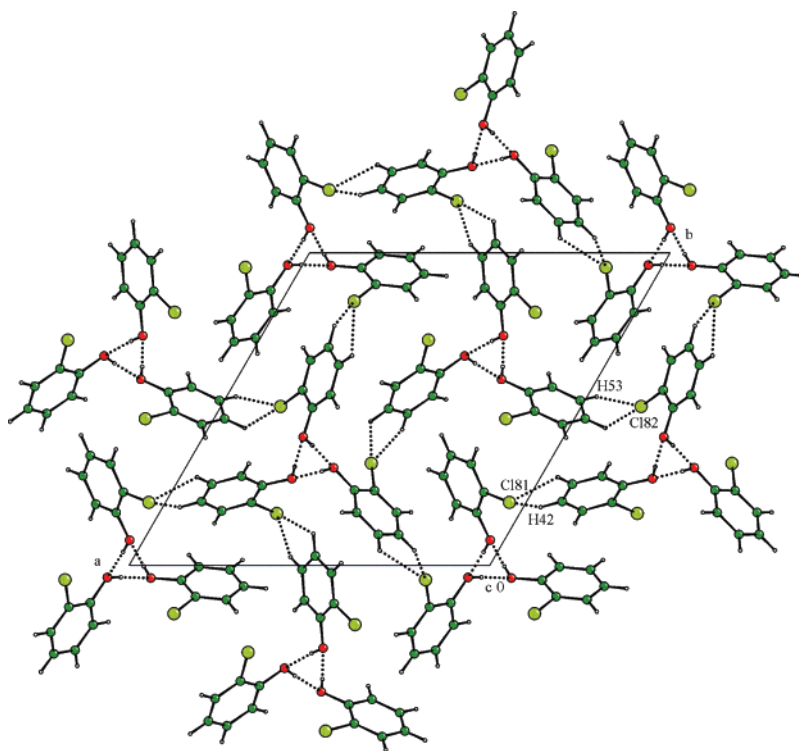


Figure 2. Crystal structure of 2-chlorophenol at ambient pressure and 100 K. Helices are formed about 3_2 axes by $\text{OH}\cdots\text{OH}$ hydrogen bond formation. The helices are linked through close contacts between the chlorine atom of one chain and two hydrogen atoms of the next. Only the shortest $\text{H}\cdots\text{Cl}$ contacts are labeled for the sake of clarity. Color scheme: C green, Cl light green, H white, O red.

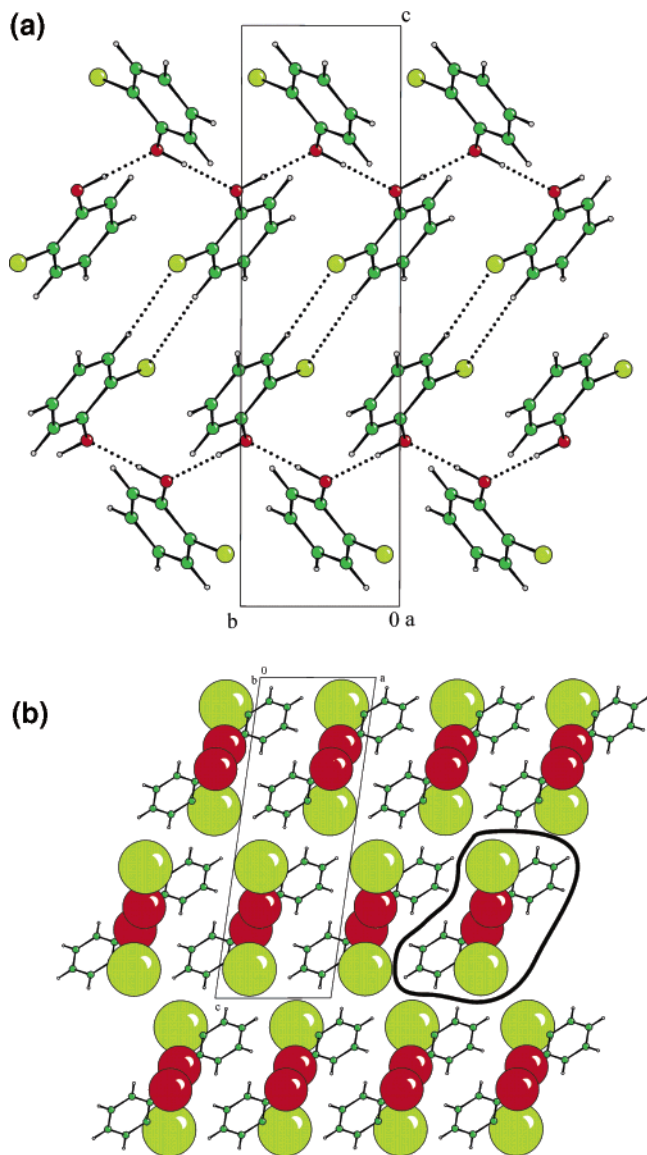


Figure 3. (a) The crystal structure of 2-chlorophenol at 0.12 GPa. The application of pressure has changed the behavior of the chlorophenyl substituent to that of a small group, allowing chains to be formed where molecules are related by a 2_1 -screw axis. Weak H \cdots Cl 'dimer' interactions are shown between the chains. (b) The ribbons (circled) lie parallel to one another over the (1 0 3) planes. This diagram shows the separation of regions of 'organic' structure by chlorine and oxygen atoms. The color scheme is the same as that in Figure 2.

2_1 screw axis (Figure 3a). The hydrogen bond connecting the equivalent molecules is actually slightly longer than in phase-I [O7 \cdots O7' measures 2.809(11) Å versus 2.748(1) – 2.762(2) Å in phase-I]. The distance between the ring centroids of neighboring molecules within a chain decreases from 5.90 Å in phase-I to 4.91 Å in phase-II. The elongation of the H-bond in phase-II relative to phase-I may therefore reflect relief of the steric interaction between the phenyl groups in this arrangement.

The H-bonded chains are connected across inversion centers by pairs of weak C3–H3 \cdots Cl8 interactions measuring 2.98 Å (the sum of the van der Waals radii of H and Cl is 2.95 Å). Similar 'dimer-like' interactions have been observed by Thalladi et al. in fluorobenzenes.⁶³

In the structure, the chains lie along the *b*-direction at $c = 1/4$ and $3/4$ and are aligned parallel to one another in the (1 0 3) planes. When the structure is viewed parallel to this, an A-B-A-B layer structure is observed where regions of chlorine and oxygen atoms are separated by the regions of carbon and hydrogen sites (Figure 3b).

4-Fluorophenol at 150 K. 4-Fluorophenol is solid at ambient temperatures and pressures and crystallizes in space group $R\bar{3}$ with one molecule in the asymmetric unit. Six molecules interact via \cdots OH \cdots OH \cdots H-bonds forming an $R_6^6(12)$ ring motif disposed about a $\bar{3}$ special position. The six-membered hydrogen-bonded $R_6^6(12)$ rings are connected together through F \cdots H interactions between H2 \cdots F8 (2.57 Å) and H5 \cdots F8 (2.65 Å). The fluorine in this structure thus acts as bifurcated acceptor for weak CH \cdots F interactions. The contact to H5 forms a dimer, which is a motif common in fluorinated benzenes (Figure 4).⁶³

The OH \cdots OH hydrogen bond at 150 K structure is the shortest to be observed in any of the monohalophenols with an O \cdots O separation of 2.650(1) Å, and we speculated that we might be able to induce a phase transition by applying pressure to a single crystal of phase-I grown ex situ. Though no phase transition was observed up to 1.7 GPa, the crystal of 4-fluorophenol developed regions of polycrystallinity over the course of 2 days, which suggests that the crystal was undergoing a phase transition, which we tentatively suggest forms phase-II (see below), though it is not possible to rule out a transition to a third phase on the basis of only our Raman data. When the pressure was released on this sample the polycrystalline regions disappeared to re-form a single crystal of 4-fluorophenol. This crystal was subsequently identified as phase-I. The process could be cycled repeatedly: on application of pressure the crystal became polycrystalline and with the release of pressure it reverted back to the single crystal.

The unit cell dimensions at 1.7 GPa showed a significant contraction along the *a*-direction but not along the *c*-direction relative to those at ambient pressure. The contraction of the *a* and *b*-axes pushes the H-bonded groups disposed about the $\bar{3}$ site closer together. The *c*-direction corresponds to a very short axis perpendicular to the H-bonded rings, so any contraction along this direction would disrupt the conformation of the six-membered hydrogen-bonded rings.

4-Fluorophenol at 0.28 GPa. Growth of a crystal of 4-fluorophenol at 0.28 GPa yields another polymorph. The new polymorph crystallizes in space group $P2_1/c$ with half a molecule in the asymmetric unit. The molecule is disordered over an inversion center.

The molecules are connected into a chain; the contact involved is presumably OH \cdots OH, as OH \cdots F is unlikely to be energetically competitive. The chains interact via F \cdots F contacts to form layers (Figure 5). Support for this view comes from the optimized (ordered) structure obtained during the crystal structure prediction study (see below). The hydrogen bonding in this structure appears to be rather long with an O7 \cdots O7' distance of 3.017(4) Å. This relatively long distance is likely to be the result of the disorder, which averages OH \cdots O(H) and F \cdots F distances. A search of the CSD for OH \cdots O(H) and C(ar)-F \cdots F–C(ar) contacts show that the mean

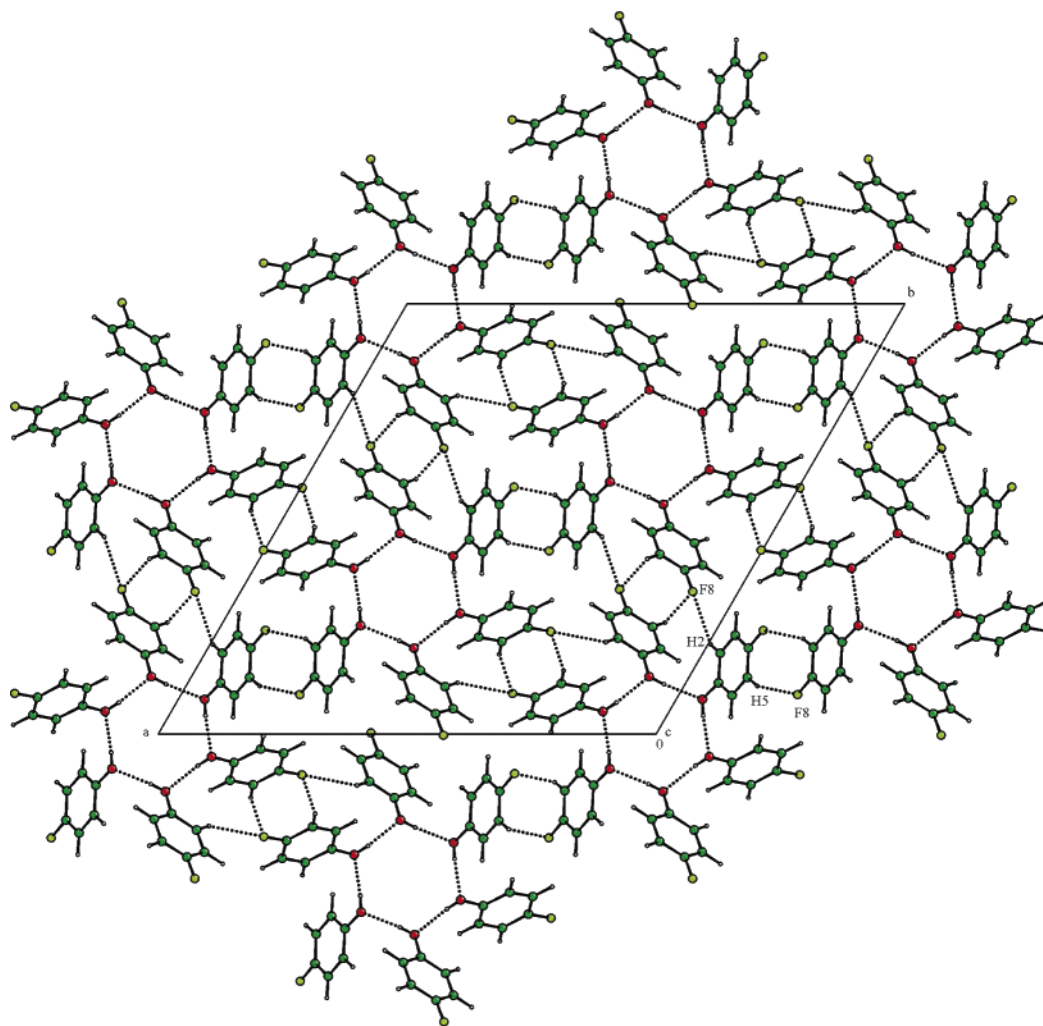


Figure 4. Crystal structure of 4-fluorophenol at 150 K viewed down the c -axis. 4-Fluorophenol crystallizes around a $\bar{3}$ special position. This type of molecular packing allows close interaction of the hydroxyl groups to form strong hydrogen bonds. The discrete hydrogen bonded motifs are connected through a dimer interaction between $H5 \cdots F8$.⁶³ F is shown in light green; otherwise, the color scheme is the same as that in Figure 2.

distance for $O \cdots O$ and $F \cdots F$ contacts are 2.78(9) and 3.1(2) Å, respectively; the average of these values is 2.94 Å.

Crystal Structure Prediction: 2-Chlorophenol.

Approximately 60 possible crystal structures of 2-chlorophenol were predicted within 5 kJ mol⁻¹ of the global minimum in lattice energy (Figure 6). Unit cell parameters, space groups, densities and energies for the 20 lowest in energy are given in Table 5. As expected, all of these lowest energy structures contain $OH \cdots O$ hydrogen bonding. About half of these form closed hydrogen-bonding rings (trimers, tetramers or hexamers), while the remainder form $OH \cdots O$ chains. 7 of the 20 lowest energy predicted crystals show the same helical hydrogen bonding as in the observed phase-I structure. However, only two of these (ranks 3 and 6 on lattice energy) form chains around a true 3-fold screw axis. The remainder make pseudo 3-fold axes in non-trigonal space groups by crystallizing with three symmetrically inequivalent molecules, as in the ambient-pressure monoclinic polymorph of phenol.

To account for the lack of kinetic considerations in the structure prediction, as well as imperfections in the model potential, we used some observations from the Cambridge Structural Database to highlight some of the

low energy predictions as being less likely than their calculated lattice energy suggests.

Many of the predicted polymorphs have very long unit cell axes ranging up to 43.4 Å, and this is unusual. The unit cell dimensions of crystal structures of molecules of less than twenty atoms crystallizing with three molecules in the asymmetric unit were extracted from the databases CSDsymmetry⁶⁴ and CSD.^{38,39} The results were plotted as a histogram (Figure 7), which showed that unit cell axes with dimensions over 30 Å are rare even with three molecules in the asymmetric unit. The rarity of such structures in the CSD could reflect a kinetic disadvantage for such elongated unit cells, perhaps because the extreme difference in repeat distances along the unit cell axes leads to extreme morphologies and uncompetitive overall growth rates. 5 of the 12 lowest structures are therefore considered to be unlikely, though not impossible, based on their unit cell dimensions.

The remaining structures are viewed with MERCURY in order to exclude any structures that have unusual intermolecular interactions. The structure corresponding to the global minimum in lattice energy lies 1.12 kJ mol⁻¹ lower than any other, but while two of the three independent molecules take part in $OH \cdots O$

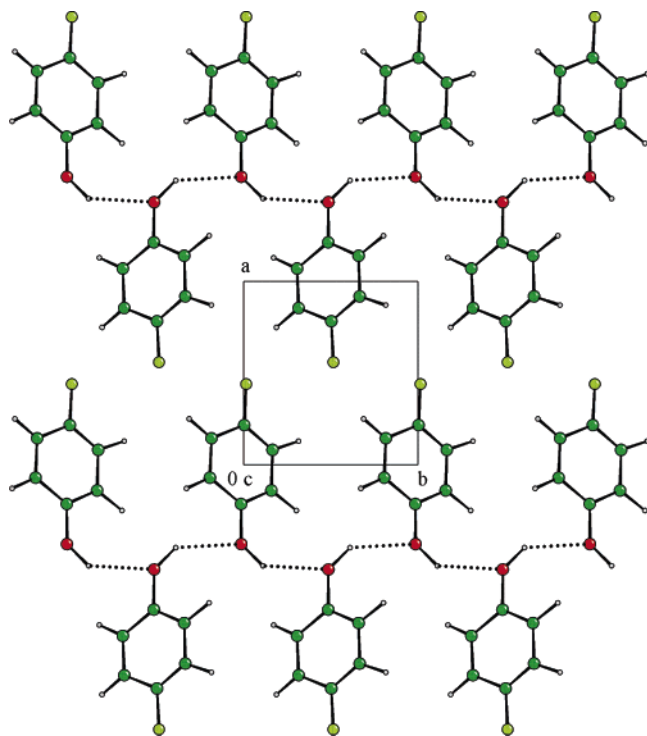


Figure 5. Crystal structure of 4-fluorophenol at 0.28 GPa viewed down the c -axis. The 4-fluorophenol molecule sits on an inversion center and is disordered about it. Only one disorder component is shown for clarity (effectively this is an ordered representation of the structure in $P2_1$). Pressure alters the behavior of the fluorophenyl group to act like a small alcohol. The chains lie parallel to each other over the $(-1\ 0\ 2)$ planes.

hydrogen-bonded chains, the third molecule instead forms $\text{OH}\cdots\text{Cl}$ chains (Figure 8). Such interactions are unlikely to be competitive with $\text{OH}\cdots\text{OH}$ chains, and the prediction of this structure could be a failing of the partly empirical model potential; the set of crystal structures used to parametrize the hydroxyl parameters did not include structures with close $\text{OH}\cdots\text{Cl}$ contacts, so the calculated energy of such interactions may be overestimated. This highlights a weakness of the empirical approach to parametrizing model potentials – uncommon interactions are poorly represented in parametrization sets and their simulation is subject to large uncertainty. Other low-energy structures take the form of hydrogen bonded trimers; a search of the CSD revealed that this motif is unusual (only 12 such structures were identified), and so structures 2 and 4 seem less likely than the other low-energy structures. From the observations above of the lowest energy structures 3, 6, 7, 10, 11 and 12 seem most reasonable.

The lowest energy structure remaining after the exclusions (No. 3) is a reasonable reproduction of the observed phase-I structure – the same structure is found by replacing the molecules in the experimental crystal structure by the gas-phase optimized molecular structure and minimizing the lattice energy. This crystal structure is the third lowest in lattice energy of the predicted structures, just $1.14\ \text{kJ mol}^{-1}$ above the global minimum. The $P2_1/c$ phase-II crystal structure was also located, as one of the densest structures located in the search – twelfth in lattice energy, $2.72\ \text{kJ mol}^{-1}$ above the global minimum, (Figure 6). It has the highest density of structures 3, 6, 7, 10, 11 and 12. We did not allow the predicted crystal structures to relax under

Table 5. Lowest Energy Predicted Structures of 2-Chlorophenol

rank on lattice energy	space group	lattice parameters				density (g cm^{-3})	lattice energy (E) (kJ mol^{-1})	$E + PV$, 1.2 kbar (kJ mol^{-1})	hydrogen bonding
		a (Å)	b (Å)	c (Å)	angles (deg)				
1	$P2_12_12_1$ ($Z' = 3$)	7.746	5.391	39.562	90	1.551	-80.36	-70.41	$\text{OH}\cdots\text{O}$ and $\text{OH}\cdots\text{Cl}$ chains
2	$P2_12_12_1$ ($Z' = 3$)	4.325	13.904	28.767	90	1.481	-79.24	-68.82	$\text{OH}\cdots\text{O}$ trimers
3^a	$P3_2$, ($Z' = 3$)	18.313	18.313	4.508	90, 90, 120	1.467	-79.22	-68.71	3-fold helical $\text{OH}\cdots\text{O}$ chains
4	$P2_12_12_1$ ($Z' = 3$)	9.452	5.554	32.980	90	1.480	-78.44	-68.02	$\text{OH}\cdots\text{OH}\cdots\text{OH}$ trimers
5	$P2_12_12_1$ ($Z' = 3$)	9.001	40.483	4.685	90	1.501	-78.35	-68.07	$\text{OH}\cdots\text{O}$ 2_1 chains
6	$P3$, ($Z' = 1$)	11.141	11.141	4.074	90, 90, 120	1.463	-78.20	-67.65	3-fold helical $\text{OH}\cdots\text{O}$ chains
7	$P2_1$ ($Z' = 3$)	4.799	10.296	17.717	90.00	1.463	-78.16	-67.62	pseudo 3-fold helical $\text{OH}\cdots\text{O}$ chains
8	$P2_12_12_1$ ($Z' = 3$)	8.447	43.358	4.830	90	1.448	-78.10	-67.45	$\text{OH}\cdots\text{O}$ and $\text{OH}\cdots\text{Cl}$ 2_1 chains
9	$P2_12_12_1$ ($Z' = 3$)	36.125	4.697	10.367	90	1.456	-77.90	-67.31	pseudo 3-fold helical $\text{OH}\cdots\text{O}$ chains
10	$P2_1$ ($Z' = 3$)	4.217	18.745	11.027	$\beta = 91.38$	1.470	-77.86	-67.37	pseudo 3-fold helical $\text{OH}\cdots\text{O}$ chains
11	$P2_12_12_1$ ($Z' = 3$)	4.834	17.895	20.306	90	1.458	-77.81	-68.50	pseudo 3-fold helical $\text{OH}\cdots\text{O}$ chains
12^b	$P2_1/c$ ($Z' = 1$)	6.538	4.788	18.666	$\beta = 103.02$	1.500	-77.64	-67.62	$\text{OH}\cdots\text{O}$ 2_1 chains
13	$P1$ ($Z' = 3$)	7.463	10.373	12.297	$\alpha = 68.68$ $\beta = 79.70$ $\gamma = 87.24$	1.468	-77.06	-66.67	$\text{OH}\cdots\text{O}$ hexamers
14	$P1$ ($Z' = 3$)	9.596	10.008	10.433	$\alpha = 114.19$ $\beta = 100.72$ $\gamma = 96.94$	1.462	-76.95	-66.82	$\text{OH}\cdots\text{O}$ hexamers
15	$P1$ ($Z' = 3$)	7.332	10.938	12.144	$\alpha = 111.88$ $\beta = 100.44$ $\gamma = 96.70$	1.471	-76.94	-66.47	$\text{OH}\cdots\text{O}$ hexamers
16	$P1$ ($Z' = 3$)	10.350	10.573	8.844	$\alpha = 109.97$ $\beta = 95.78$ $\gamma = 104.35$	1.485	-76.94	-66.39	$\text{OH}\cdots\text{O}$ hexamers
17	$P2_1$ ($Z' = 1$)	6.883	4.819	8.769	$\beta = 100.33$	1.492	-76.69	-66.27	$\text{OH}\cdots\text{O}$ 2_1 chains
18	$P2_12_12_1$ ($Z' = 3$)	4.170	32.195	12.997	90	1.468	-76.68	-66.35	pseudo 3-fold helical $\text{OH}\cdots\text{O}$ chains
19	$P2_1/c$ ($Z' = 2$)	12.747	7.847	14.743	$\beta = 127.77$	1.465	-76.68	-66.34	$\text{OH}\cdots\text{O}$ tetramers
20	$P1$ ($Z' = 2$)	7.718	7.907	10.282	$\alpha = 95.49$ $\beta = 94.25$ $\gamma = 113.40$	1.501	-76.67	-66.17	$\text{OH}\cdots\text{O}$ tetramers

^a Corresponds to the experimentally observed phase-I. ^b Corresponds to the experimentally observed phase-II.

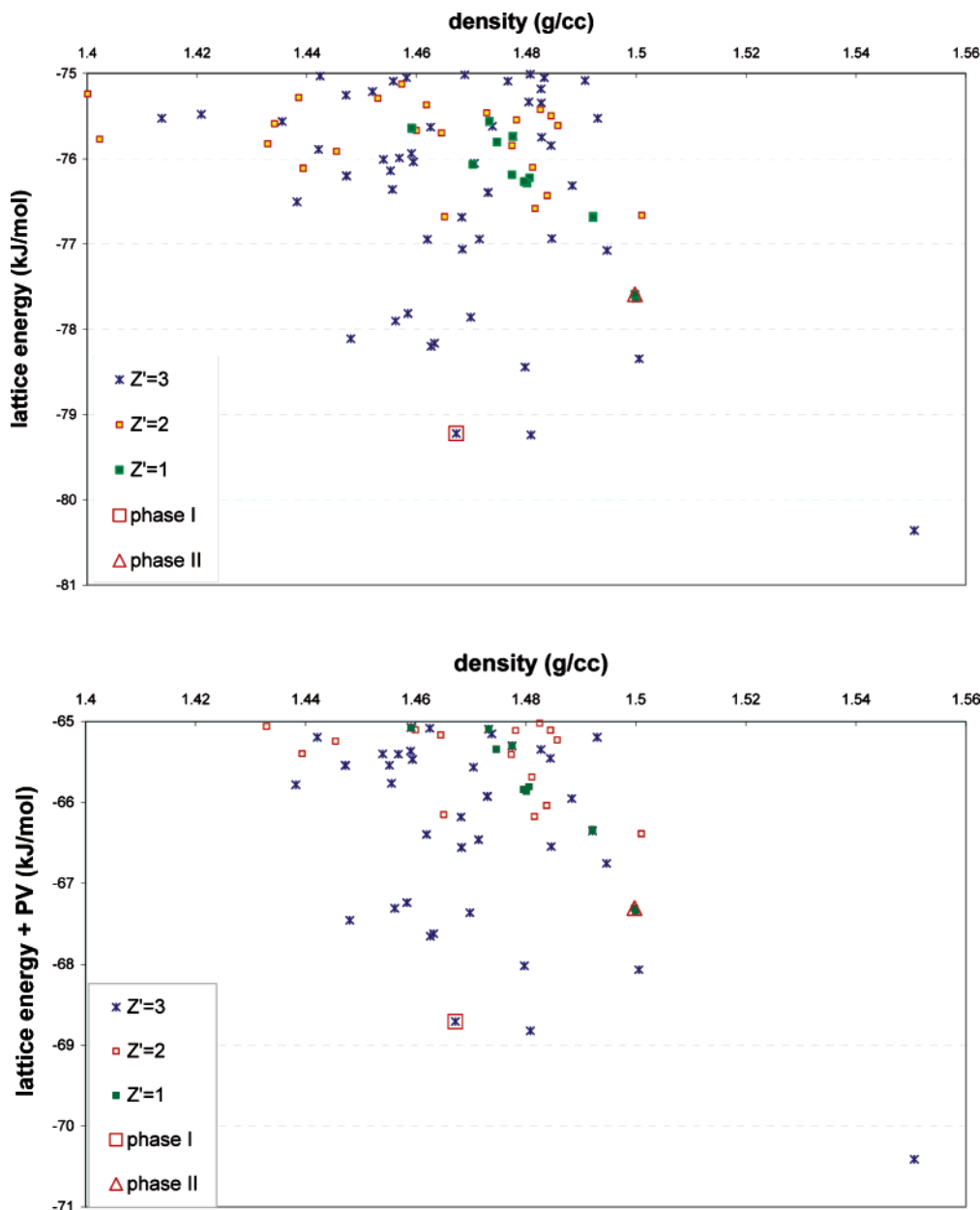


Figure 6. Plot of lattice energy against density for the predicted structures of 2-chlorophenol within 5 kJ mol⁻¹ of the global minimum (top) and of lattice energy + *PV* at 0.12 GPa (bottom).

pressure (this feature is not yet implemented in the code), but estimated the effect of the high pressure by adding the *PV* contribution to the energy at 0.12 GPa. The *PV* term favors the higher density structures and improves the ranking of the high-pressure phase-II structure, which has the eighth lowest lattice energy + *PV* among the predicted structures.

The predictions were performed with a rigid planar molecular structure, while the hydroxyl group in the experimentally observed structures is distorted significantly out of the plane of the aromatic ring, presumably to optimize hydrogen bonding interactions in the crystal. To test the effect of this molecular distortion, we energy-minimized the phase-I and II structures with the hydroxyl out-of-plane angle fixed at the experimentally observed values (8.1°, 13.4° and 19.1° for molecules 1, 2 and 3 in phase-I, and 21.7° in phase-II). The results of these minimizations (Tables 6 and 7) demonstrate the effect of the assumed molecular structure on the model-

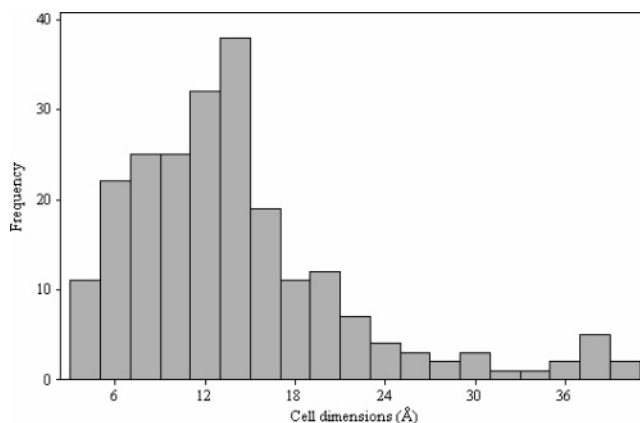


Figure 7. Distribution of the cell dimensions for crystal structures of molecules with twenty atoms or less crystallizing with three molecules in the asymmetric unit extracted from CSDsymmetry⁶⁴ and CSD.^{38,39}

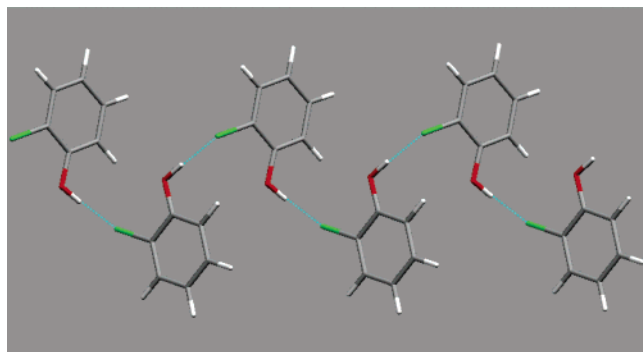


Figure 8. OH...Cl chains in the global minimum predicted structure of 2-chlorophenol. These are not expected to be energetically competitive with OH...OH hydrogen bonds and their presence in this structure may reflect the parametrization of the potential used.

ing of these structures. For phase-I, the lattice energy minimized structure is improved dramatically with the torsion angles fixed to the experimental values – the RMS error in the lattice parameters, a , b and c are decreased from 17.7% with the planar molecular structure down to 2.2% with the experimentally observed torsion angle. While the crystal structure is very sensitive to the orientation of the hydroxyl groups, the lattice energy is nearly unaffected (Table 6). The phase-II lattice energy minimum with the hydroxyl group torsion angle fixed at 21.7° is in slightly worse agreement with the experimentally observed structure than the crystal structure calculated with the planar molecular structure (Table 7). However, in this case, the lattice energy is decreased significantly and the density is increased slightly; the molecular distortion appears to have an important stabilizing effect on this crystal structure.

Crystal Structure Prediction: 4-Fluorophenol.

The predictions for 4-fluorophenol produced structures with similar packing motifs as the 2-chlorophenol predictions; about half of the 20 lowest energy structures (Table 8) form closed hydrogen-bonded rings, while the rest show OH...O chain motifs (Figure 9).

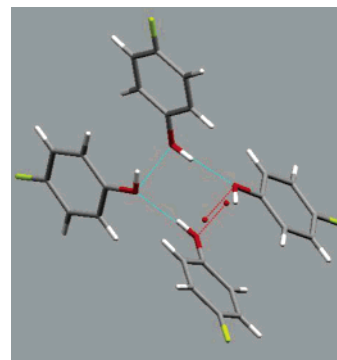


Figure 9. Four-fold chains in the global minimum predicted structure of 4-fluorophenol.

The lattice energy was minimized to yield the observed phase-I crystal structure with the molecular structure replaced by the planar model used in the search (Table 9); the resulting structure matches exactly to the 15th lowest energy predicted crystal, 1.25 kJ mol^{-1} above the global minimum. We also energy minimized this model with the hydroxyl out-of-plane torsion angle set to the observed value of 9° ; the unit cell dimensions are almost unaffected by this change, while the lattice energy is lowered by more than 1 kJ mol^{-1} (Table 9).

The prediction methodology can only generate ordered crystal structures, so the high-pressure polymorph of 4-fluorophenol could not be predicted exactly. However, the 10th lowest energy predicted structure is an ordered version of the observed phase-II – the same lattice energy minimum (Table 10) is found by replacing the disordered molecular structure in the observed crystal by the planar molecular model, fixed in one of the two orientations (as in Figure 5). As with 2-chlorophenol, this high-pressure crystal is among the densest of the predicted structures. As a result, the PV contribution to the energy favors this crystal over most of the other predictions (Table 8 and Figure 10).

Such sensitivity of the lattice energy to small changes in the molecular structure prevents any better results

Table 6. Lattice-Energy-Minimized Unit Cells of the Ambient-Pressure Crystal Structure of 2-Chlorophenol

	$a = b$ (Å)	c (Å)	volume (Å ³)	lattice energy (kJ mol ⁻¹)
expt	16.072	5.896	1318.9	
Lattice Energy Minima				
with gas phase (planar) molecular structure	18.313 (+13.9%)	4.508 (-23.5%)	1309.5 (-0.7%)	-79.22
with experimentally observed torsion angles ^a	16.311 (+1.49%)	5.708 (-3.19%)	1315.2 (-0.29%)	-79.14

^a The lattice energy minimized crystal structure with the hydroxyl group out-of-plane torsion angles adjusted to the experimentally observed values (-8.1° , -13.4° , -19.1°).

Table 7. Lattice-Energy-Minimized Unit Cells of the High-Pressure Crystal Structure of 2-Chlorophenol

	a (Å)	b (Å)	c (Å)	β (deg)	volume (Å ³)	lattice energy (kJ mol ⁻¹)
expt	6.464	4.909	18.131	98.11	569.57	
Lattice Energy Minima						
with gas phase (planar) molecular structure	6.538 (+1.14%)	4.788 (-2.46%)	18.666 (+2.95%)	103.02 (+5.00%)	569.36 (-0.04%)	-77.64
With experimentally observed torsion angle ^a	6.465 (+0.01%)	4.563 (-7.05%)	19.201 (+5.90%)	94.65 (-3.53%)	564.55 (-0.88%)	-82.44

^a The lattice energy minimized crystal structure with the hydroxyl group out-of-plane torsion angle adjusted to the experimentally observed value (21.7°).

Table 8. Lowest Energy Predicted Structures of 4-Fluorophenol

structure	space group	lattice parameters				density (g cm ⁻³)	lattice energy (<i>E</i>) (kJ mol ⁻¹)	<i>E</i> + <i>PV</i> , 1.2 kbar (kJ mol ⁻¹)	hydrogen bonding
		<i>a</i> (Å)	<i>b</i> (Å)	<i>c</i> (Å)	angles (deg)				
1	<i>P</i> ₂ ₁ ₂ ₁ 2 ₁ (<i>Z'</i> = 2)	5.617	21.687	8.871	90	1.3780	-63.37	-40.59	pseudo 4-fold helical OH...O chains
2	<i>P</i> ₂ ₁ / <i>c</i> (<i>Z'</i> = 2)	19.744	11.423	4.540	$\beta = 82.92$	1.3747	-63.16	-40.33	OH...O tetramers
3	<i>P</i> 1 (<i>Z'</i> = 2)	4.907	10.137	11.042	$\alpha = 85.06$ $\beta = 86.30$ $\gamma = 82.78$	1.3735	-62.91	-40.06	OH...O tetramers
4	<i>P</i> ₂ ₁ / <i>c</i> (<i>Z'</i> = 2)	8.069	15.243	8.862	$\beta = 90.86$	1.3664	-62.83	-39.86	OH...O 2 ₁ chains
5	<i>Pca</i> 2 ₁ (<i>Z'</i> = 3)	19.705	4.991	16.456	90	1.3803	-62.52	-39.78	pseudo 3-fold helical OH...O chains
6	<i>P</i> ₂ ₁ (<i>Z'</i> = 3)	9.489	16.685	5.201	$\beta = 88.42$	1.3568	-62.48	-39.35	pseudo 3-fold helical OH...O chains
7	<i>P</i> ₂ ₁ ₂ ₁ 2 ₁ (<i>Z'</i> = 2)	22.896	8.245	5.711	90	1.3813	-62.46	-39.74	pseudo 4-fold helical OH...O chains
8	<i>Pna</i> 2 ₁ (<i>Z'</i> = 3)	10.669	8.714	17.986	90	1.3358	-62.44	-38.94	OH...OH...F...OH pseudo 4-fold chains
9	<i>P</i> ₂ ₁ / <i>c</i> (<i>Z'</i> = 2)	12.499	20.137	4.845	$\beta = 116.12$	1.3601	-62.33	-39.25	OH...O tetramers
10	<i>P</i>₂₁ (<i>Z'</i> = 1)^b	8.115	5.346	6.438	$\beta = 106.40$	1.3893	-62.26	-39.67	OH...O 2₁ chains
11	<i>P</i> ₃ ₂ (<i>Z'</i> = 3)	15.796	15.796	6.101	90,90,120	1.2708	-62.23	-37.53	pseudo 3-fold helical OH...O chains
12	<i>C</i> 2/ <i>c</i> (<i>Z'</i> = 3)	20.417	10.402	16.242	$\beta = 97.83$	1.3074	-62.21	-38.20	OH...O hexamers
13	<i>P</i> ₂ ₁ (<i>Z'</i> = 3)	6.037	9.181	15.854	90,00	1.2710	-62.19	-37.49	pseudo 3-fold helical OH...O chains
14	<i>P</i> ₃ ₁ (<i>Z'</i> = 1)	9.183	9.183	6.016	90,90,120	1.2713	-62.17	-37.48	3-fold helical OH...O chains
15	<i>R</i>₃ (<i>Z'</i> = 1)^a	22.264	22.264	5.934	90,90,120	1.3154	-62.12	-38.26	OH...O hexamers
16	<i>P</i> 1 (<i>Z'</i> = 2)	7.332	8.127	10.437	$\alpha = 83.32$ $\beta = 73.91$ $\gamma = 67.65$	1.3475	-62.09	-38.80	OH...O tetramers
17	<i>P</i> ₂ ₁ (<i>Z'</i> = 2)	8.767	5.501	11.398	$\beta = 102.69$	1.3885	-62.07	-39.46	OH...O 2 ₁ chains
18	<i>P</i> 1 (<i>Z'</i> = 2)	7.436	8.100	9.249	$\alpha = 95.41$ $\beta = 98.99$ $\gamma = 94.70$	1.3660	-61.99	-39.01	OH...O tetramers
19	<i>P</i> 1 (<i>Z'</i> = 2)	8.124	7.909	8.773	$\alpha = 99.80$ $\beta = 94.76$ $\gamma = 92.71$	1.3477	-61.95	-38.66	OH...O tetramers
20	<i>P</i> ₂ ₁ (<i>Z'</i> = 2)	7.922	5.502	12.772	$\beta = 105.16$	1.3858	-61.93	-39.28	OH...O 2 ₁ chains

^a Corresponds to the experimentally observed phase-I. ^b Corresponds to the experimentally observed phase-II.

Table 9. Lattice-Energy-Minimized Unit Cells of the Ambient-Pressure Crystal Structure of 4-Fluorophenol

	<i>a</i> = <i>b</i> (Å)	<i>c</i> (Å)	volume (Å ³)	lattice energy (kJ mol ⁻¹)
expt	22.620	5.569	2467.7	
Lattice Energy Minima				
with gas phase (planar) molecular structure	22.263 (-1.58%)	5.935 (+6.56%)	2547.4 (+3.2%)	-62.12
with experimentally observed torsion angles ^a	22.294 (-1.44%)	5.925 (+6.39%)	2550.4 (+3.4%)	-63.42

^a The lattice energy minimized crystal structure with the hydroxyl group out-of-plane torsion angle adjusted to the experimentally observed value (9.0°).

Table 10. Lattice-Energy-Minimized Unit Cell of an Ordered Model of the High-Pressure Crystal Structure of 4-Fluorophenol

	<i>a</i> (Å)	<i>b</i> (Å)	<i>c</i> (Å)	β (deg)	volume (Å ³)	lattice energy (kJ mol ⁻¹)
expt	6.281	5.724	7.798	106.06	267.98	
lattice energy minimum	6.438 (+2.51%)	5.346 (-6.60%)	8.115 (+4.06%)	106.40 (+0.32%)	267.98 (-0.53%)	-62.26

with the rigid body approximation than achieved here (i.e. the observed structure within 1–2 kJ mol⁻¹ of the global minimum). This means that selection of likely structures from the list presented in Table 8 is more difficult than in 2-chlorophenol, though a few structures (e.g. 7, 8, 9 and 11) can be ruled out by the presence on unreasonable OH...F or O...O intermolecular interactions. We note, though, that almost none of the unobserved predicted polymorphs contain the common H...F motifs described by Thalladi et al.,⁶³ and it may be that there is some room for improvement of methodologies for modeling weak H...halogen interactions.

Discussion

Crystal Packing at Low-Temperature and High Pressure. Packing in the crystal structure of monoal-

cohols was investigated first by Brock and Duncan⁶⁵ and subsequently by Taylor and Mcrae.⁶⁶ Both studies showed that the size of the R-group attached to the alcohol functionality is a major factor in the packing behavior of the molecules. When the R-group is small then the molecules are usually related by a 2₁ screw axis or a glide plane. If the R-group is bulky then the molecules tend to aggregate around 3-, 4- or 6-fold screw, rotation or rotoinversion axes. These operations may be crystallographic – i.e. crystallization occurs in a high-symmetry space group – or noncrystallographic, implying that crystallization occurs in a low-symmetry space group with *Z'* > 1.

At ambient pressure 2-chlorophenol and 4-fluorophenol behave typically for alcohols with bulky R-groups. Both form structures containing molecules connected by

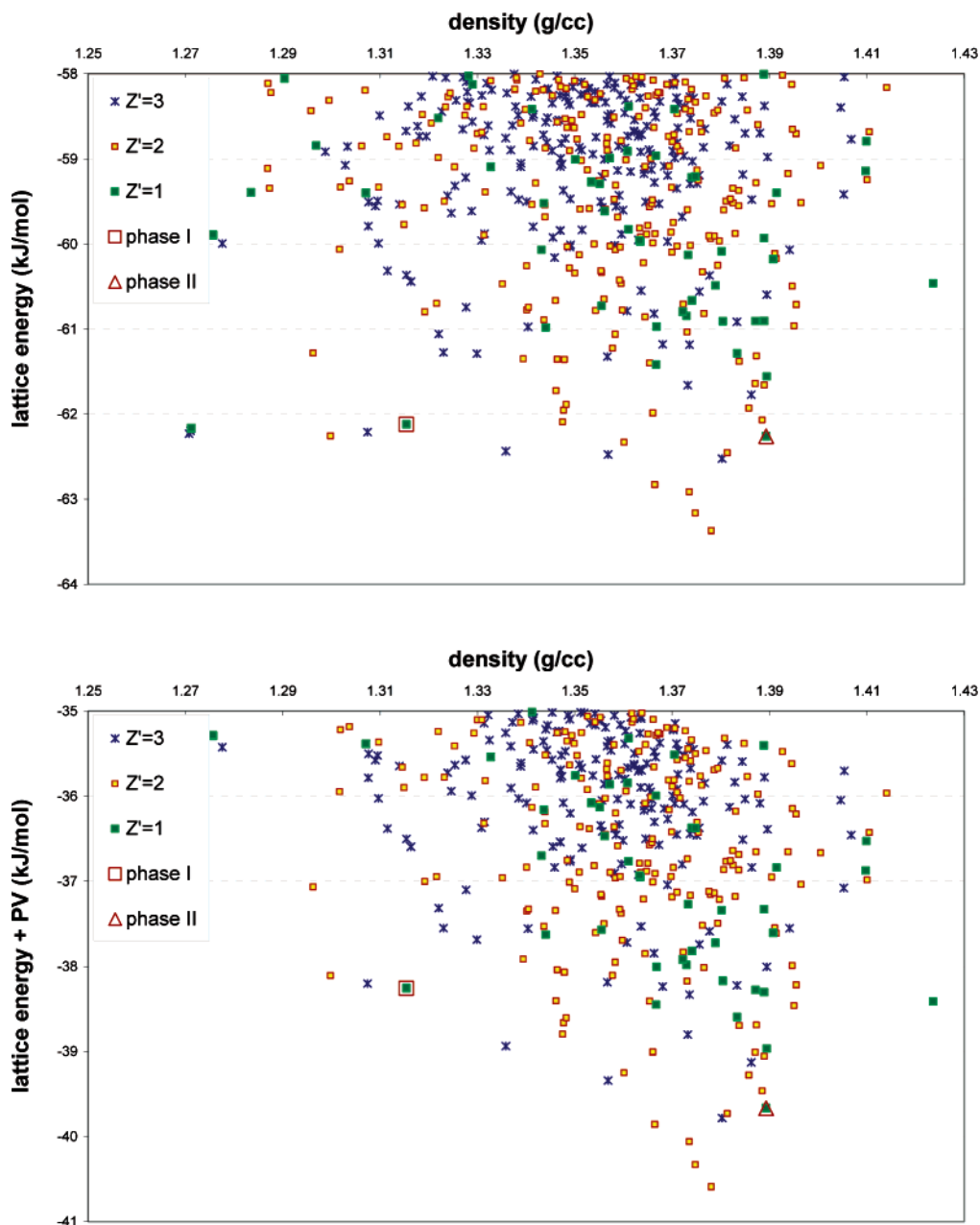


Figure 10. Plot of lattice energy against density for the predicted structures of 4-fluorophenol within 5 kJ mol^{-1} of the global minimum (top) and of lattice energy + PV at 0.28 GPa (bottom).

$\text{OH}\cdots\text{OH}\cdots$ interactions. At ambient pressure, chains are formed in 2-chlorophenol about a crystallographic 3_2 screw axes. In 4-fluorophenol the molecules hydrogen bond to form rings about 3 rotoinversion sites. On application of pressure, however, the structures change to ones in which the chains lie along a 2_1 screw axes. In effect, pressure has altered the packing behavior of the halophenyl groups from being characteristic of a large group to more typical of a small group.

We have recently shown that, rather unusually for simple alcohols, the other monofluoro- and chlorophenols display quite complicated packing motifs.¹⁶ We have only been able in those cases to examine the effects of pressures up to 0.36 GPa (a modest figure by the standards of modern high-pressure crystallography), and it remains to be seen what happens to those systems at higher pressures. The alteration in packing behavior is observed in phenol itself, however.⁶ Phase-I

crystallizes at ambient pressure in space group $P2_1$ with three molecules in the asymmetric unit; these H-bond together to form a pseudo 3-fold helix (Figure 11a). At high pressure (0.16 GPa) another structure with $Z' = 3$ in $P2_1$ is obtained, the structure consisting of two crystallographically independent chains. The first chain is formed about a 2_1 screw axis, while the second comprises two independent molecules disposed about a pseudo 2_1 screw axis (Figure 11b).

Although alcohols tend to crystallize about screw axes, Brock and Duncan⁶⁵ recognized that it should, in principle, be possible to generate hydrogen bonded chains by simple translation in the case of a very small alcohol. They cited no examples of where this has been observed, however. In fact, the effect of high pressure on the crystal structure of methanol^{3,67} can also be interpreted in terms of a shift from small alcohol packing to very small alcohol packing. This is illustrated

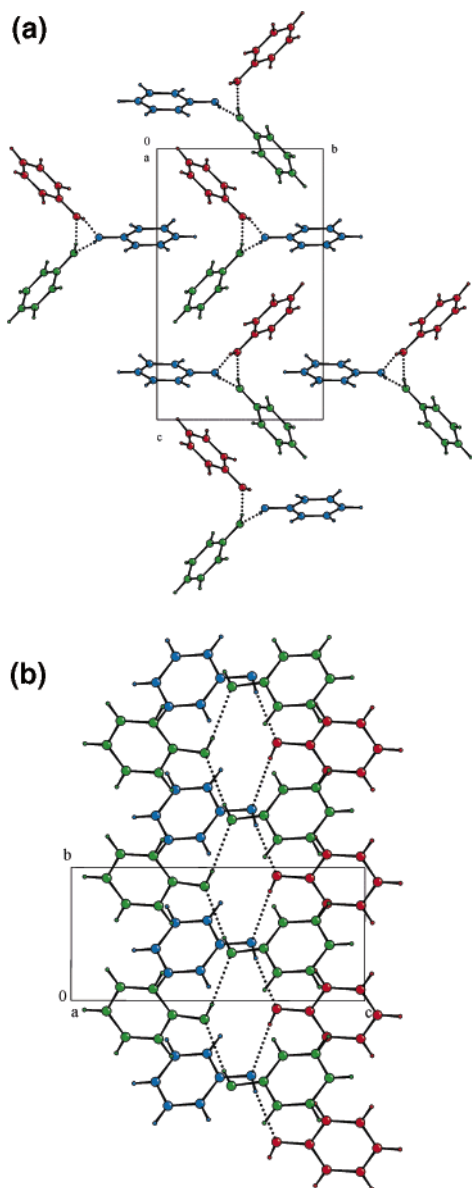


Figure 11. (a) The crystal structure of phenol⁶ at ambient pressure and 123 K. The phenyl ring acts like a bulky substituent. It crystallizes with three molecules in the asymmetric unit that emulate a 3-fold helix along b in the low-symmetry space group $P2_1$. (b) Phenol at 0.16 GPa. The behavior of the phenyl group resembles that of a small substituent, with symmetry equivalent molecules related by crystallographic or pseudo- 2_1 screw axes. There are three molecules in the asymmetric unit with the blue and red molecules forming a pseudo- 2_1 screw axis and the green molecules forming a chain where the molecules are related by a crystallographic 2_1 screw axis.

in Figure 12: at ambient pressure and 163 K the crystal structure of methanol contains chains of molecules that are related by a glide plane in an alternating 1–1–1 motif (Figure 12a).⁶⁷ At 7 GPa the high-pressure polymorph exhibits chains forming a 2–1–2–1 motif with three molecules in the asymmetric unit (Figure 12b). The pairs of molecules on the same side of the hydrogen bonded chains in Figure 12b are related by a pseudo-translation, confirming Brock and Duncan's intuitive argument.

Despite the change in packing behavior in alcohols with application of high pressure, the size of the group

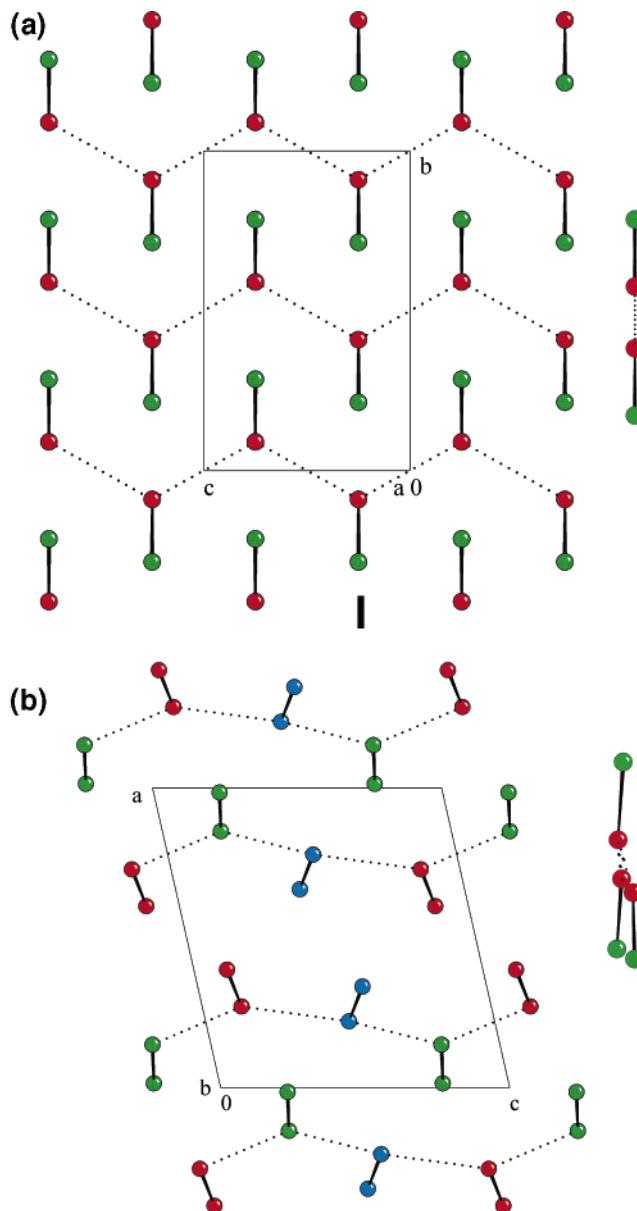


Figure 12. (a) Ambient-pressure phase of methanol⁶⁷ at 163 K showing packing behavior typical of a small monoalcohol: symmetry-equivalent molecules are related by a c -glide in a 1:1:1 sequence (i.e. one molecule on one side of the chain, one on the other, and so on). (b) At pressure (7 GPa) methanol³ undergoes a phase transition to three molecules in the asymmetric unit in a 2–1–2–1 sequence. Color-coding represents crystallographic equivalence. To the right of the main diagrams, is shown a projection along the chains in each of the phases. The pseudo translational symmetry can be seen in the high-pressure phase. The bulky methyl group is preventing the molecules from coming closer together to form perfect translational symmetry.

is important in determining the lengths of intermolecular interactions. In the OH \cdots OH chains of 2-chlorophenol the intermolecular O \cdots O distances are longer at 0.12 GPa than at ambient pressure [2.817(16) Å versus 2.748(1) to 2.762(2) Å at 100 K]. The elongation of the hydrogen bond can be seen in 4-fluorophenol where the O7 \cdots O7' distance is 2.650(1) Å at 150 K and about 3 Å at 0.28 GPa (it is not possible to be precise because of the O/F disorder in that structure).

This increase in hydrogen bond lengths is also observed in other high-pressure phases of alcohols. The

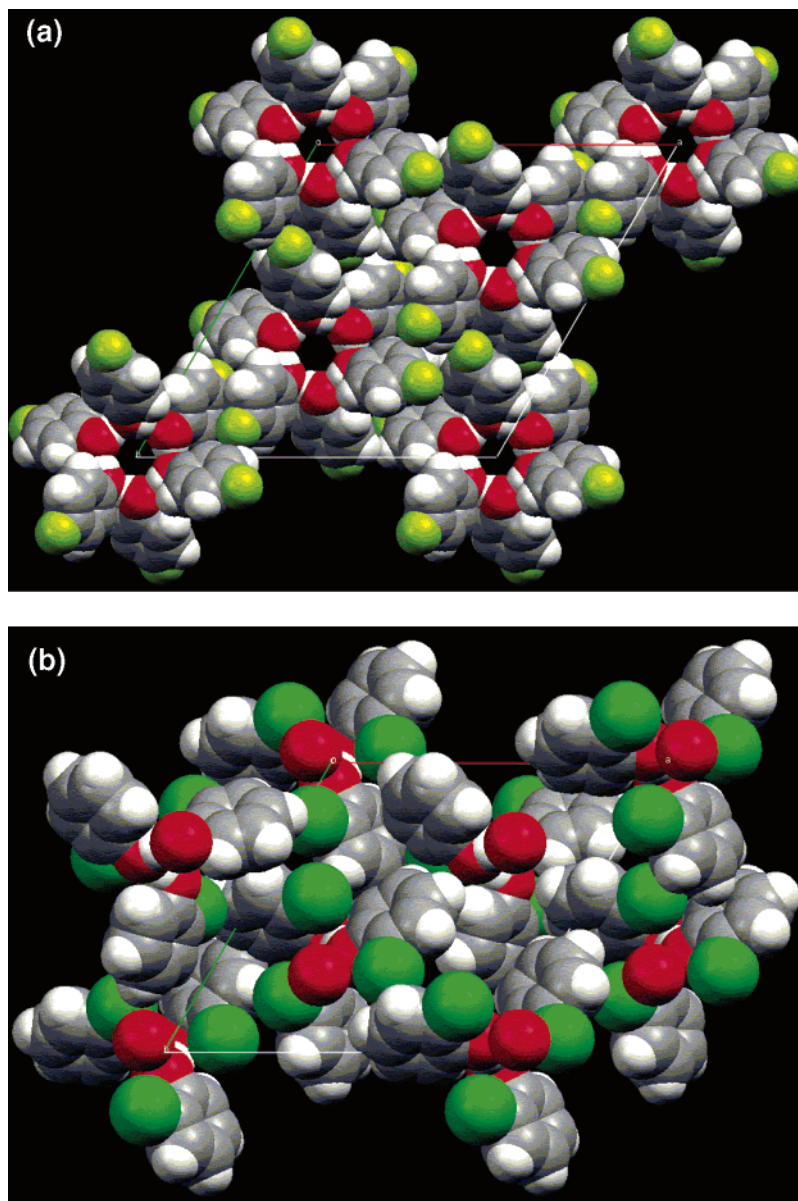


Figure 13. (a) The space filling diagram of 4-fluorophenol. The voids present in the structure are clearly seen running down the *c*-direction. (b) The space filling diagram of 2-chlorophenol. The voids in this structure are present between the symmetry inequivalent helices. High-pressure crystal growth of these two compounds induces molecular rearrangement to a denser structure without voids.

crystal structure of phenol has three different hydrogen bonds in both the ambient- and high-pressure phases. All three hydrogen bonds show an increase in length from an average of 2.671 Å at ambient pressure to 2.964 Å at high pressure. The high-pressure phase of phenol shows both forms of molecular aggregation in the formation of the two crystallographically unique chains as discussed previously. Interestingly, the H-bond used in the chain formed from symmetry equivalent molecules disposed about a 2_1 axis is longer than the others (disposed about a pseudo 2_1 axis); crystallographically inequivalent molecules that are H-bonded into a chain can deviate from exact symmetry to accommodate the large R-groups while minimizing the O \cdots O distance.

In methanol at ambient pressure the O \cdots O distance is 2.67 Å. At 7 GPa, O \cdots O distances between molecules on opposite sides of the chain (i.e. those which bear a similar spatial relationship to the molecules in the

ambient-pressure structure) decrease to 2.43 Å and 2.52 Å, while the H-bond that connects molecules on the same side of the chain elongates to 2.70 Å.

That intermolecular contacts should lengthen under pressure is counter-intuitive, but this occurs in order to accommodate the bulkier R-group in the 'small monoalcohol' packing arrangement. The preference for 'small alcohol packing' at high pressure is a consequence of the higher densities that appear to be achievable with these motifs. Inspection of space-filling plots of the high and low-pressure phases described here shows that the low-temperature phases are both characterized by the presence of voids. The voids present in the crystal structure of 2-chlorophenol are much less obvious than those in 4-fluorophenol but are formed between the helices formed along the *c*-axis (Figure 13). It has recently been shown that the effects of pressure on the crystal structures of amino acids can also be understood

by compression of the voids present at ambient pressure.^{9,10} Similar conclusions have recently been reached by Slebodnick et al. in a compression study of Ru₃(CO)₁₂.⁶⁸ The voids are found to contract under pressure until intermolecular interactions become so short that the structure becomes unstable; then a phase transition occurs. This effect often leads to destructive phase transitions, but the advantage of studying low melting compounds is denser polymorphs are formed at the time of crystal growth. This has occurred in the two compounds in this study (Table 1).

Crystal Structure Predictions. The low- and high-pressure polymorphs of both halophenols were predicted among the lowest in lattice energy and within a few kJ mol⁻¹ of the lowest energy predicted structures. In both cases, the two forms have similar calculated lattice energies and the high-pressure form was predicted as one of the densest possible crystal structures.

Although elaborate models for the intermolecular energy were used, we cannot expect to calculate relative stabilities any better than a few kJ mol⁻¹, given the lack of entropy and explicitly including pressure effects in the energy minimizations. Furthermore, the position of the hydroxyl hydrogen is influenced by the crystal environment, twisting the hydroxyl group up to about 20° out of the plane of the molecule. Thus, the rigid molecule assumption also limits the possible accuracy of the crystal structure prediction.

The results of the crystal structure prediction are especially encouraging because of the success in locating the 2-chlorophenol crystal structure with three symmetrically independent molecules – predicting structures with more than one molecule in the asymmetric unit is one of the major challenges for crystal structure prediction methods.¹⁵ Many of the methods used to search for possible crystal structures are extendible to multiple molecules and it is mainly a matter of the large increase in computing time required for such searches.

Disordered structures are another challenge for crystal structure prediction. Although current methodologies only predict perfectly ordered crystal structures, such predictions can be useful in interpreting disordered crystals.⁵⁷ Here, the packing of some of the lowest energy structures of 4-fluorophenol hinted that disorder is possible in crystals of this molecule. More systematic approaches to predicting disorder in crystals have shown promise when there is a suspicion that such behavior may be important.⁶⁹

Conclusions

High pressure is potentially a very valuable tool for tuning the balance between intermolecular interactions such as hydrogen bonding and van der Waals interactions. In this paper we have shown that the packing behavior of 2-chlorophenol and 4-fluorophenol can be transformed from being characteristic of bulky alcohols to that of small alcohols. We have shown that this trend is also followed by phenol and methanol. The transition from bulky to small behavior under high pressure is accompanied by an increase in hydrogen bonding distances; this counter-intuitive effect occurs in order to optimize packing.

Crystal structure predictions almost always generate more hypothetical structures than known polymorphs,

and we hypothesized that high pressure could be a useful method of accessing some of the structures that are not observed under ambient conditions; this view is supported by the results of this study. However, energy-ordering is sensitive to assumed intramolecular conformation; halogen...H interactions also seem to be poorly modeled. We are currently unable to energy-minimize structures under applied pressure, and this was treated in an approximate way. These are evidently serious problems with the approach used here. Nevertheless, the observed low-temperature and high-pressure structures did appear among the lowest energy predicted structures, even though one of these had $Z' = 3$. This is a very encouraging result indeed. Furthermore, many proposed structures could be ruled-out through comparison to known structures in the Cambridge Structural Database – e.g. because they exhibited unusual patterns of intermolecular interactions. Though it is clearly not yet possible to draw a general conclusion on the ability of current methodologies to predict high-pressure crystal structures, our results should encourage the further combined use of extreme conditions and computational approaches to the study of polymorphism and intermolecular interactions in crystals.

Acknowledgment. We thank the EPSRC, the Cambridge Crystallographic Data Centre, the Pfizer Institute for Pharmaceutical Materials Science, and the University of Edinburgh for funding.

Supporting Information Available: Crystallographic information files (CIF) for all structures reported here. This material is available free of charge via the Internet at <http://pubs.acs.org>.

References

- (1) Lommerse, J. P. M.; Motherwell, W. D. S.; Ammon, H. L.; Dunitz, J. D.; Gavezzotti, A.; Hofmann, D. W. M.; Leusen, F. J. J.; Mooji, W. T. M.; Price, S. L.; Schweizer, B.; Schmidt, M. U.; van Eijck, B. P.; Verwer, P.; Williams, D. E. *Acta Crystallogr. Sect. B* **2000**, *56*, 697–714.
- (2) Motherwell, W. D. S.; Ammon, H. L.; Dunitz, J. D.; Dzyabchenko, A.; Erk, P.; Gavezzotti, A.; Hofmann, D. W. M.; Leusen, F. J. J.; Lommerse, J. P. M.; Mooji, W. T. M.; Price, S. L.; Scheraga, H.; Schweizer, B.; Schmidt, M. U.; van Eijck, B. P.; Verwer, P.; Williams, D. E. *Acta Crystallogr. Sect. B* **2002**, *58*, 647–661.
- (3) Allan, D. R.; Clark, S. J.; Brugmans, M. J. P.; Ackland, G. J.; Vos, W. L. *Phys. Rev. B* **1998**, *58*, R11809–R11812.
- (4) Allan, D. R.; Clark, S. J. *Phys. Rev. B* **1999**, *60*, 6328–6334.
- (5) Allan, D. R.; Parsons, S.; Teat, S. J. *J. Synchrotron Radiat.* **2001**, *8*, 10–17.
- (6) Allan, D. R.; Clark, S. J.; Dawson, A.; McGregor, P. A.; Parsons, S. *Acta Crystallogr. Sect. B* **2002**, *58*, 1018–1024.
- (7) Allan, D. R.; Clark, S. J.; Parsons, S.; Ruf, M. *J. Phys.: Condensed Matter* **2000**, *12*, L613–L620.
- (8) Allan, D. R.; Clark, S. J.; Ibberson, R. M.; Parsons, S.; Pulham, C. R.; Sawyer, L. *Chem. Commun.* **1999**, 751–752.
- (9) Dawson, A.; Allan, D. R.; Belmonte, S. A.; Clark, S. J.; David, W. I. F.; McGregor, P. A.; Parsons, S.; Pulham, C. R.; Sawyer, L. *Cryst. Growth Des.*, submitted for publication, 2004.
- (10) Moggach, S. A.; Allan, D. R.; Morrison, C. A.; Parsons, S.; Sawyer, L. *Acta Crystallogr. Sect. B* **2005**, *61*, 58–68.
- (11) Beyer, T.; Day, G. M.; Price, S. L. *J. Am. Chem. Soc.* **2001**, *123*, 5086–5094.
- (12) Anghel, A. T.; Day, G. M.; Price, S. L. *CrystEngComm.* **2002**, *4*, 348–355.
- (13) Perrin, P. M.; Michel, P. *Acta Crystallogr. Sect. B* **1973**, *29*, 253–258.
- (14) Perrin, P. M.; Michel, P. *Acta Crystallogr. Sect. B* **1973**, *29*, 258–263.

- (15) Day, G. M.; Motherwell, W. D. S.; Ammon, H.; Boerrigter, S. X. M.; Della Valle, R. G.; Venuti, E.; Dzyabchenko, A. V.; Dunitz, J. D.; van Eijck, B. P.; Erk, P.; Facelli, J. C.; Bazterra, V. E.; Ferraro, M. B.; Hofmann, D. W. M.; Leusen, F. J. J.; Liang, C.; Pantelides, C. C.; Karamertzanis, P. G.; Price, S. L.; Lewis, T. C.; Torrisi, A.; Nowell, H.; Scheraga, H. A.; Arnautova, Y. A.; Schmidt, M. U.; Schweizer, B.; Verwer, P. Manuscript in preparation, 2004.
- (16) Oswald, I. D. H.; Allan, D. R.; Motherwell, W. D. S.; Parsons, S. *Acta Crystallogr. Sect. B* **2005**, *61*, 69–79.
- (17) Cosier, J.; Glazer, A. M. *J. Appl. Crystallogr.* **1986**, *19*, 105–107.
- (18) Boese, R.; Nussbaumer, M. In *Correlations, Transformations, and Interactions in Organic Crystal Chemistry*, Jones, D. W., Katrusiak, A., Eds.; Crystallographic Symposia 7, International Union of Crystallography, Chester, U.K. 1994; pp 20–37.
- (19) Bruker-Nonius. *SMART* version 5.624. Bruker-AXS, Madison, WI, 2001.
- (20) Bruker-Nonius. *SAINTE* version 7. Bruker-AXS, Madison, WI, 2003.
- (21) Sheldrick, G. M. *SADABS Version 2004–1*. Bruker-AXS, Madison, WI, 2004.
- (22) Blessing, R. H. *Acta Crystallogr. Sect. A* **1995**, *51*, 33–38.
- (23) Altomare, A.; Casciarano, G.; Giacovazzo, C.; Guagliardi, A. *J. Appl. Crystallogr.* **1993**, *26*, 343–350.
- (24) Betteridge, P. W.; Carruthers, J. R.; Cooper, R. I.; Prout, K.; Watkin, D. J. *J. Appl. Crystallogr.* **2003**, *36*, 1487.
- (25) Flack, H. D. *Acta Crystallogr. Sect. A* **1983**, *39*, 876–881.
- (26) Merrill, L.; Bassett, W. A. *Rev. Sci. Instrum.* **1974**, *45*, 290–294.
- (27) Sparks, R. A. *GEMINI*. Version 1.01, Bruker-AXS, Madison, WI, 2000.
- (28) Parsons, S. *SHADE*. The University of Edinburgh, U.K., 2004.
- (29) Blessing, R. H. *J. Appl. Crystallogr.* **1997**, *30*, 421–426.
- (30) Dawson, A.; Allan, D. R.; Parsons, S.; Ruf, M. *J. Appl. Crystallogr.* **2004**, *37*, 410–416.
- (31) Shankland, K.; David, W. I. F. In *Structure Determination from Powder Diffraction Data*, David, W. I. F., Shankland, K., McCusker, L. B., Baerlocher, Ch., Eds. IUCr Monographs on Crystallography, No. 13, Oxford University Press: Oxford, U.K., 2002, pp 252–285.
- (32) Bruker-Nonius. *TOPAS V3.0: General Profile and Structure Analysis Software for Powder Diffraction Data*, 2004.
- (33) Sheldrick, G. M. *SHELXTL-XP* version 6.01. University of Göttingen, Germany and Bruker-Nonius Inc., Madison, WI, 2001.
- (34) Bruno, I. J.; Cole, J. C.; Edgington, P. R.; Kessler, M.; Macrae, C. F.; McCabe, P.; Pearson, J.; Taylor, R. *Acta Crystallogr. Sect. B* **2002**, *58*, 389–397.
- (35) Watkin, D. J.; Pearce, L.; Prout, C. K. *CAMERON – A Molecular Graphics Package*. Chemical Crystallography Laboratory, University of Oxford, England, 1993.
- (36) Spek, A. L. *J. Appl. Crystallogr.* **2003**, *36*, 7–13.
- (37) Farrugia, L. J. *J. Appl. Crystallogr.* **1999**, *32*, 837–838.
- (38) Allen, F. H. *Acta Crystallogr. Sect. B* **2002**, *58*, 380–388.
- (39) Allen, F. H.; Motherwell, W. D. S. *Acta Crystallogr. Sect. B* **2002**, *58*, 407–422.
- (40) Karfunkel, H. R.; Gdanitz, R. J. *J. Comput. Chem.* **1992**, *13*, 1171–1183.
- (41) Karfunkel, H. R.; Leusen, F. J. J.; Gdanitz, R. J. *J. Comput.-Aided Mater. Design* **1994**, *1*, 177–185.
- (42) Verwer, P.; Leusen, F. J. J. *Rev. Comput. Chem.* **1998**, *12*, 327–365.
- (43) Accelrys Inc. *CERIUS2* version 4.6, San Diego, CA, 2001.
- (44) Vosko, S. J.; Wilk, L.; Nusair, M. *Can. J. Phys.* **1980**, *58*, 1200–1211.
- (45) Becke, A. D. *J. Chem. Phys.* **1988**, *88*, 2547–2553.
- (46) Perdew, J. P.; Wang, Y. *Phys. Rev. B* **1992**, *45*, 13244–13249.
- (47) Delley, B. *J. Chem. Phys.* **1990**, *92*, 508–517.
- (48) Williams, D. E. *J. Mol. Struct.* **1999**, *486*, 321–347.
- (49) Williams, D. E. *J. Comput. Chem.* **2001**, *22*, 1–20.
- (50) Hsu, L.-Y.; Williams, D. E. *Acta Crystallogr. Sect. A* **1980**, *36*, 277–281.
- (51) Williams, D. E.; Houpt, D. J. *Acta Crystallogr. Sect. B* **1986**, *42*, 286–295.
- (52) Amos, R. D.; with contributions from Alberts, I. L.; Andrews, J. S.; Colwell, S. M.; Handy, N. C.; Jayatilaka, D.; Knowles, P. J.; Kobayashi, R.; Koga, N.; Laidig, K. E.; Maslen, P. E.; Murray, C. W.; Rice, J. E.; Sanz, J.; Simandiras, E. D.; Stone, A. J.; Su, M.-D. *CADPAC*, 6.0 ed., Cambridge, 1995.
- (53) Stone, A. J. *Chem. Phys. Lett.* **1981**, *83*, 233–239.
- (54) Stone, A. J.; Alderton, M. *Mol. Phys.* **1985**, *56*, 1047–1064.
- (55) Munowitz, M. G.; Wheeler, G. L.; Colson, S. D. *Mol. Phys.* **1977**, *34*, 1727–1737.
- (56) Day, G. M.; Price, S. L. *J. Am. Chem. Soc.* **2003**, *125*, 16434–16443.
- (57) Tremayne, M.; Grice, L.; Pyatt, J. C.; Seaton, C. C.; Kariuki, B. M.; Tsui, H. H. Y.; Price, S. L.; Cherryman, J. C. *J. Am. Chem. Soc.* **2004**, *126*, 7071–7081.
- (58) Day, G. M.; Chisholm, J.; Shan, N.; Motherwell, W. D. S.; Jones, W. *Cryst. Growth Des.* **2004**, *4*, 1327–1340.
- (59) Willock, D. J.; Price, S. L.; Leslie, M.; Catlow, C. R. A. *J. Comput. Chem.* **1995**, *16*, 628–647.
- (60) Price, S. L.; Willock, D. J.; Leslie, M.; Day, G. M. *DMAREL* version 3.1, University College London, London, U.K., 2001.
- (61) Chisholm, J.; Motherwell, W. D. S. *J. Appl. Crystallogr.*, submitted for publication.
- (62) Steiner, T. *Angew. Chem., Int. Ed.* **2002**, *41*, 48–76.
- (63) Thalladi, V. R.; Weiss, H.-C.; Blaser, D.; Boese, R.; Nangia, A.; Desiraju, G. R. *J. Am. Chem. Soc.* **1998**, *120*, 8702–8710.
- (64) Yao, J. W.; Cole, J. C.; Pidcock, E.; Allen, F. H.; Howard, J. A. K.; Motherwell, W. D. S. *Acta Crystallogr. Sect. B* **2002**, *58*, 640–646.
- (65) Brock, C. P.; Duncan, L. L. *Chem. Mater.* **1994**, *6*, 1307–1312.
- (66) Taylor, R.; Macrae, C. F. *Acta Crystallogr. Sect. B* **2001**, *57*, 815–827.
- (67) Tauer, K. J.; Lipscomb, W. N. *Acta Crystallogr.* **1952**, *5*, 606–612.
- (68) Slebodnick, C.; Zhao, J.; Angel, R.; Hanson, B. E.; Song, J.; Liu, Z.; Hemley, R. J. *Inorg. Chem.* **2004**, *43*, 5245–5252.
- (69) van Eijck, B. P. *Phys. Chem. Chem. Phys.* **2002**, *4*, 4789–4794.